Heterogeneous Virus Strategies Promote Coexistence in Virus-Microbe Systems

Hayriye Gulbudak[1,*] and Joshua S. Weitz[2,3]

[1] *Department of Mathematics, University of Louisiana at Lafayette, Lafayette, Louisiana, USA*
[2] *School of Biological Sciences, Georgia Institute of Technology, Atlanta, GA, USA*
[3] *School of Physics, Georgia Institute of Technology, Atlanta, GA, USA*

(Dated: September 18, 2017)

Viruses of microbes, including bacterial viruses (phage), archaeal viruses, and eukaryotic viruses, can influence the fate of individual microbes and entire populations. Here, we model distinct modes of virus-host interactions and study their impact on the abundance and diversity of both viruses and their microbial hosts. We consider two distinct viral populations infecting the same microbial population via two different strategies: lytic and chronic. A lytic strategy corresponds to viruses that exclusively infect and lyse their hosts to release new virions. A chronic strategy corresponds to viruses that infect hosts and then continually release new viruses via a budding process without cell lysis. The chronic virus can also be passed on to daughter cells during cell division. The long-term association of virus and microbe in the chronic mode drives differences in selective pressures with respect to the lytic mode. We utilize invasion analysis of the corresponding nonlinear differential equation model to study the ecology and evolution of heterogenous viral strategies. We first investigate stability of equilibria, and characterize oscillatory and bistable dynamics in some parameter regions. Then, we derive fitness quantities for both virus types and investigate conditions for competitive exclusion and coexistence. In so doing we find unexpected results, including a regime in which the chronic virus requires the lytic virus for survival and invasion.

I. INTRODUCTION

Viruses of microbes such as bacterial viruses (phage), archaeal viruses, and eukaryotic viruses, have a substantial impact on the ecosystem. Interactions between microbes and their viruses affect competition between distinct host and virus types which in turn impacts the ecological community and biodiversity among microbial cells and viruses []. For example, microbial populations can evolve resistance to infection from certain phages or microbial cells can gain immunity through CRISPR, either one modulating the structure and dynamics of the microbe-phage community [3]. The abundance and diversity of these viruses, along with microbes whom they infect, are well documented. The interactions between viruses and their microbial hosts play a central role in maintenance of the virus-microbial biodiversity and the phenotypic properties displayed by species in virus-microbial communities [5, 9, 15, 20].

Distinct physiological states, life strategies and adaptations emerge in response to the frequent interactions between viruses and microbes. For example, bacteria have evolved adaptive immunity [], and they also display bet-hedging heterogeneous phenotypic strategies such as dormancy [2, 11]. Microbial viruses can exploit their hosts with different strategies, such as lytic, lysogenic, and chronic, which vary in virulence to their hosts. Lytic and lysogenic are the most commonly studied viral infection modes. Virulent viruses reproduce only by destroying their hosts (lytic) and temperate viruses are additionally capable of multiplying as intracellular parasites with the same cell lineage (lysogenic). In some cases, a virus can be temperate for one host and virulent for another [10**?**]. The chronic infection mode is much less understood. In chronic state, the virus neither integrates into the host genome nor induces lysis. Instead, the virus forms a persistent infection where progeny are routinely budded off the cell or passed down to daughter cells asymmetrically after division. In this paper, we focus on how the chronic infection viral strategy impacts the diversity and population dynamics displayed in a virus-microbial host community, from a theoretical modeling perspective.

In our system, microbial cells gain immunity to lytic virus through chronic viral infection, leading to a long-lived infected cell state with distinct vital parameters from the susceptible cells. The distinct reproducing cell types, chronic and susceptible, compete for limited resources which are consumed by the total microbial population (chronic, susceptible and lytic infected). The competitive host-host and virus-virus interactions along with host-virus predator-prey relationships result in a complex web of interactions which together determine the ecological and evolutionary outcomes of the microbe-virus system.

Many theoretical studies exclusively focus on lytic type infection and try to address how inter- and intra-species interactions impact the dynamics of both viruses and their microbial hosts [1, 5–7]. For example, researchers have studied the effect of limited resources on the population dynamics of microbial or virus strains in the paradigm of coexistence or exclusion of species [8]. Competing bacteria and viruses may persist together due to predator-mediated coexistence when multiple bacteria and viral species with varying resistance and virulence, respectively, are present [3**?**]. However with a single

*Electronic address: hayriye.gulbudak@louisiana.edu

microbial host type and co-infection or superinfection of a single cell prevented (via viral induced superinfection exclusion or superinfection immunity), theoretical and experimental evidence point to the competitive exclusion principle for competing lytic virus [].

Costs and benefits of differing viral infection modes have been shown to influence dynamics, for example temperate virus may provide infected host cell immunity against more virulent viruses[**?**], yet infection may have fitness costs for microbial hosts [4]. Lytic infecting virus act as predators of microbes, decreasing host population fitness [15]. Chronically infecting viruses, some way analogous to temperate viruses, may prevent infected cells against subsequent lytic viral infection (superinfection exclusion) [**?**], and also carry costs evidenced by the variety of resistance mechanisms that hosts display against them [15]. Yet it is unclear how the two distinct infection modes, lytic and chronic, affect the diversity of viral populations displaying each strategy, along with the fitness of their common host. In this work, our results suggest that the heterogeneity in the infection modes promotes coexistence among the distinct viral populations.

Here, we develop a system of differential equations modeling the complex interactions between lytic and chronic viruses with their common host population. In order to investigate the interaction of multiple virus types, we first analyze infection dynamics of the chronic viral infection mode, which turns out to be of interest in its own right. In particular, several complex bifurcations, distinct from lytic infection dynamics, are found and analyzed. Then we investigate how lytic and chronically infecting virus strains interact together with their common host population, and the resulting impact on the abundance, biodiversity of both viruses and their host. Through analytical and numerical methods, we determine the parameter regimes and underlying mechanisms leading to coexistence or exclusion of distinct virus types. In so doing we find interesting results on the effect of heterogeneous virus strategies, including a regime in which the chronic virus requires the virulent lytic virus for survival and invasion. Finally, we link our results to evolutionary trajectory of virulence in virus infecting microbial hosts.

II. METHODS

Here we propose a model of virus-host interactions. The model describes the dynamics of interactions between multiple virus strains and one type host. In the model, $S(t), I(t), C(t)$ represent the number of susceptible, infected, chronically infected cells at time t, respectively, and $V_L(t), V_C(t)$ depict the density of free lytic and chronically infecting virus particles, respectively. We assume that during infective process, the lytic (or chronically infecting) virus is absorbed and infects the susceptible cells with a rate ϕ (or $\tilde{\phi}$). If lytic infection takes place, a number of hosts cells lysis with a rate η and produce *viable* virions with an effective virus multiplicity rate β. If chronic infection takes place, chronically infecting viruses produce progeny, which are slowly budded off the cell with a rate α or passed down to daughter cells and divide with a rate $\tilde{r}(1-\frac{N}{K})$ without cell lysis at any time. Cells die with a rate d and viruss decay with a rate μ. Chronic infection is costly; so we assume that chronic infection process shortens the life span of cells so that chronically infected cells die with a rate $\tilde{d}(\geq d)$.

A nonlinear differential equation systems that describes the interactions and the dynamics of host and virus populations can be written as follows:

$$
\begin{aligned}
\text{Susceptible} \quad \frac{\mathrm{d}S}{\mathrm{d}t} &= \overbrace{rS(1-\frac{N}{K})}^{\text{logistic growth}} - \overbrace{S(\phi V_L + \tilde{\phi} V_C}^{\text{absorption}} - \overbrace{dS}^{\text{death}} \\
\text{Infected} \quad \frac{\mathrm{d}I}{\mathrm{d}t} &= \overbrace{\phi S V_L}^{\text{infection}} - \overbrace{dI}^{\text{natural death}} - \overbrace{\eta I}^{\text{death due to lysis}} \\
\text{Lytic virus} \quad \frac{\mathrm{d}V_L}{\mathrm{d}t} &= \overbrace{\beta \eta I}^{\text{virus production due to lysis}} - \overbrace{\phi S V_L}^{\text{absorption}} \\
&\quad - \overbrace{\mu V_L}^{\text{viral decay}} , \\
\text{Chro. Inf.} \quad \frac{\mathrm{d}C}{\mathrm{d}t} &= \overbrace{\tilde{r}C(1-\frac{N}{K})}^{\text{chro. inf. logistic growth}} + \overbrace{\tilde{\phi} S V_C}^{\text{chronic inf.}} \\
&\quad - \overbrace{\tilde{d}C}^{\text{natural death}} \\
\text{Chronic virus} \quad \frac{\mathrm{d}V_C}{\mathrm{d}t} &= \overbrace{\alpha C}^{\text{virus prod. due to budding}} - \overbrace{\tilde{\phi} S V_C}^{\text{absorption}} \\
&\quad - \overbrace{\mu V_C}^{\text{viral decay}} ,
\end{aligned}
\tag{I}
$$

where N is the total number of cells, $N = S + I + C$.

We do not consider co-infection or superinfection due to cross immunity provided by each viral infection against the other strain (superinfection exclusion []). In particular, we assume that when infection of a host cell with two virus particles takes place, competition between virus particles in a cell for a limited amount of key enzyme more often results in exclusion of all but one of them (*key enzyme* hypothesis [10]). The logistic term in cell growth rate depicts the competition between infected and susceptible cells for limited resources with carrying capacity K.

In Section IV, we study the outcome of competing lytic and chronic strains on virus-host ecology and evolution in model (I). First we explore and summarize infection dynamics under each type of virus infection

mode separately, in section (III), which will also facilitate analysis of the multi-strain model.

III. INFECTION DYNAMICS

A. Lytic Infection Dynamics

First we reduce the system of equations (I) to a three-dimensional system by taking $V_C(t) = 0$ and $C(t) = 0$, in other words we consider the following subsystem with only lytic viral infection:

$$\begin{aligned} \frac{\mathrm{d}S}{\mathrm{d}t} &= rS(1-\frac{N}{K}) - \phi S V_L - dS \\ \frac{\mathrm{d}I}{\mathrm{d}t} &= \phi S V_L - (d+\eta)I \\ \frac{\mathrm{d}V_L}{\mathrm{d}t} &= \beta\eta I - \phi S V_C - \mu V_L. \end{aligned} \tag{II}$$

Previous results suggest that lytic virus-host interactions results in three distinct asymptotic outcomes (assuming $r > d$): virus clearance, steady state or oscillatory dynamics [1]. Indeed, the lytic subsystem (II) has an infection-free equilibrium,

$$\mathcal{E}_0 = (S_0, 0, 0)\,, \ \textit{where } S_0 = K(1-\frac{d}{r}), \tag{1}$$

and persistence versus extinction depends upon the lytic infection threshold $\mathcal{R}_0^L$:

$$\mathcal{R}_0^L = \frac{\phi S_0}{\phi S_0 + \mu}\frac{\beta\eta}{(\eta+d)}.$$

The reproduction number $\mathcal{R}_0^L$ is formulated differently than the threshold derived in [1], but both formulas are equivalent as threshold quantities. Here, the biological interpretation of $\mathcal{R}_0^L$ is the average number of secondary cases (infected with lytic viruses) produced by one infected cell (or virus) during its life span in a wholly susceptible microbial cell population. The first term $\dfrac{\phi S_0}{\phi S_0 + \mu}$ is the probability of a virus infecting a cell before decaying and the second term $\dfrac{\beta\eta}{(\eta+d)}$ quantifies the average number of new viruses produced by one infected cell in its lifetime. Berretta and Kuang [1] show (in a rescaled version of (II)) the following: If $\mathcal{R}_0^L < 1$, the lytic virus population eventually dies out and the susceptible cell population converges to the equilibrium S_0. Otherwise if $\mathcal{R}_0^L > 1$, the virus (*uniformly*) persists and the populations converge to the positive equilibrium $\mathcal{E}_+ = (S_L^+, I_L^+, V_L^+)$, with

$$S_L^+ = \frac{\mu(\eta+d)}{\phi(\beta\eta-(\eta+d))}, \tag{2}$$

$$I_L^+ = \frac{\mu V_L^+}{(\beta\eta-(\eta+d))}, \tag{3}$$

$$V_L^+ = \frac{r(\eta+d)(\phi S_0+\mu)(\mathcal{R}_0^L-1)}{\phi(\mu r + K\phi(\beta\eta-(\eta+d)))}. \tag{4}$$

if it is locally asymptotically stable. Yet under certain conditions, this equilibrium $\mathcal{E}_+$ loses its stability through Hopf bifurcation, in which case both virus-hosts populations undergo sustained oscillations [1] (see Fig. 1).

B. Chronic Infection Outcomes

Next, we consider the subsystem of the model (I) where $V_L(t) = 0$ and $I(t) = 0$, which describes the interactions and the dynamics of host and chronically infecting virus populations:

$$\begin{aligned} \frac{\mathrm{d}S}{\mathrm{d}t} &= rS(1-\frac{N}{K}) - \tilde{\phi} S V_C - dS \\ \frac{\mathrm{d}C}{\mathrm{d}t} &= \tilde{r}C(1-\frac{N}{K}) + \tilde{\phi} S V_C - \tilde{d}C \\ \frac{\mathrm{d}V_C}{\mathrm{d}t} &= \alpha C - \tilde{\phi} S V_C - \mu V_C, \end{aligned} \tag{III}$$

where N is the total number of cells, $N = S + C$. Both lytic-only and chronic-only subsystems have the same infection-free equilibrium, $\mathcal{E}_0$, characterized by S_0, the equilibrium level of susceptible cells in the absence of infection. Utilizing the Next Generation Matrix Approach (see Appendix VII B 1), we obtain the reproduction number of chronically infecting virus $\mathcal{R}_0^C$:

$$\mathcal{R}_0^C = \frac{\tilde{r}}{\tilde{d}}(1-\frac{S_0}{K}) + \frac{\tilde{\phi} S_0}{\tilde{\phi} S_0 + \mu}\frac{\alpha}{\tilde{d}}.$$

The threshold, $\mathcal{R}_0^C$, gives the average number of secondary chronically infected cells produced by one chronically infected cell during the life span in a wholly susceptible cell population. The first term $\dfrac{\tilde{r}}{\tilde{d}}(1-\dfrac{S_0}{K})$ is *the average number of offsprings* produced by an average chronically infected cell during its life span (through vertical transmission) and the second term $\dfrac{\tilde{\phi} S_0}{\tilde{\phi} S_0 + \mu}\dfrac{\alpha}{\tilde{d}}$ describes the average number of secondary chronically infected cases produced by one chronically infected cell during its life span among completely susceptible cell population (through horizontal transmission). Notice the additional first term compared with the lytic reproduction number $\mathcal{R}_0^C$. So even in the absence of horizontal chronic infection ($\tilde{\phi} = 0$), chronic viruses and infected cells can persist

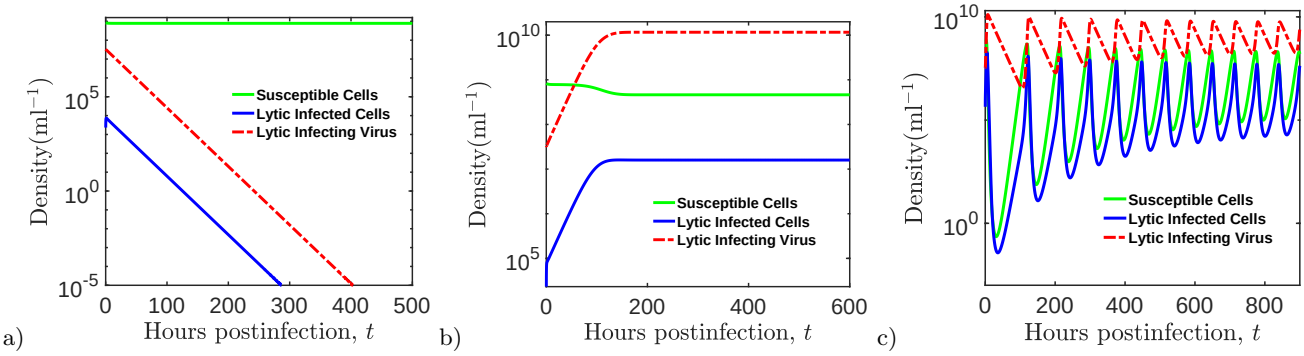

FIG. 1: Dynamics of the lytic-subsystem (II) with the density of susceptible hosts, $S(t)$, lytic infected hosts, $I(t)$, and lytic infecting free viruses, $V_L(t)$, at time t. a) Infection dies out and solutions converge to infection-free equilibrium $\mathcal{E}_0$. b) Solutions converge to steady-state equilibrium $\mathcal{E}_L^+$. c) Stable positive equilibrium, $\mathcal{E}_L^+$, undergoes Hopf bifurcation and solutions present sustainable oscillations, converging to a limit cycle. Common parameters for the dynamics are given in the Table III. The initial virus and host densities are $V_0^L = 0.04 \times S_0$ viruses/ml, $S_0 = 8.3 \times 10^8$ hosts/ml. For part (a) $\phi = .0.1 \times 10^{-11}$, part (b) $\phi = 0.1 \times 10^{-10}$ and part (c) $\phi = 0.55 \times 10^{-9.5}$ with $\eta = 1.5$.

so long as:

$$\mathcal{R}_0^C = \frac{\tilde{r}}{\tilde{d}}(1 - \frac{S_0}{K}) > 1.$$

The chronic subsystem (III) exhibits more possible *boundary* equilibria than the lytic subsystem (II). There is the infection-free equilibrium $\mathcal{E}_0$ as defined for the lytic subsystem (1). In addition, there can be another boundary equilibrium, namely a chronic-only equilibrium given by

$$\mathcal{E}_c = (0, C_0, V_c), \quad \text{with} \quad C_0 = K(1 - \frac{\tilde{d}}{\tilde{r}}) \text{ and } V_c = \frac{\alpha}{\mu} C_0, \tag{5}$$

which exists when $\tilde{d} < \tilde{r}$. The chronic subsystem (III) also can have one or two positive *interior* equilibrium,

$$\mathcal{E}_{C,i}^+ = (S_{C,i}^+, C_{C,i}^+, V_{C,i}^+), \qquad \text{where} \tag{6}$$

$$\begin{aligned} S_{C,i}^+ &= \frac{-a_1 \pm \sqrt{a_1^2 - 4a_0 a_3}}{2a_0}, \\ C_{C,i}^+ &= (B - \frac{r}{\tilde{r}}) S_{C,i}^+ + \frac{\mu}{\tilde{\phi} S_0} B, \\ V_{C,i}^+ &= \frac{\alpha C_{C,i}^+}{\tilde{\phi} S_{C,i}^+ + \mu}, \end{aligned} \tag{7}$$

with

$$\begin{aligned} a_0 &= \tilde{\phi}(B - \frac{r}{\tilde{r}} + 1) \\ a_1 &= (B - \frac{r}{\tilde{r}} + 1)\mu + \tilde{\phi}(\frac{\mu}{\tilde{\phi}} B - C_0 - \frac{K\alpha}{\tilde{r}}) \\ a_2 &= \mu(\frac{\mu}{\tilde{\phi}} B - C_0) \end{aligned}$$

and $B = (\frac{r}{K\alpha}(S_0 - C_0))$ (for derivations, see Appendix VII C 2). Finally, the trivial *community collapse equilibrium*, $\mathcal{E}_0^0 = (0, 0, 0)$, always exists, but is unstable as long as $r > d$. For the rest of the paper, we assume $r > d$, which is a necessary and sufficient condition for existence of the infection-free equilibrium $\mathcal{E}_0 = (S_0, 0, 0)$.

Given all possible equilibria of the chronic subsystem, the stability analysis of the system (III) provide us crucial information for the complex dynamics displayed by the system (III). Analytical results suggest that, provided by Theorem VII.1 in Appendix (VII B 1), if $\mathcal{R}_0^C < 1$, then $\mathcal{E}_0$ is locally asymptotically stable. Yet, this does not guarantee extinction of the virus for all initial conditions. In particular, there are parameter regimes with *bistable dynamics* or *bistability*, which generally refers to a dynamical system containing multiple stable equilibria and/or limit cycles with distinct basins of attraction [22]. In other words, the initial virus or infected cell density affects to which attractor the solution converges.

A condition for occurrence of bistability can be analytically expressed as a local condition at $\mathcal{R}_0^C = 1$. Considering $\tilde{r}$ as a bifurcation parameter, bistability occurs when the critical bifurcation point ($\tilde{r} = \tilde{r}_c, C_C^+ = 0$), where $\mathcal{R}_0^C(\tilde{r}_c) = 1$, satisfies

$$\left(\left[B(\tilde{r}_c) - \frac{r}{\tilde{r}_c} + 1 \right] \left[\frac{\mu r}{\tilde{\phi} \tilde{r}_c} \right] + \frac{\alpha K}{\tilde{r}_c} + C_0(\tilde{r}_c) \right) > 0 \tag{8}$$

with $C_0(\tilde{r}_c) = K(1 - \frac{\tilde{d}}{\tilde{r}_c})$, and $B(\tilde{r}_c) = \frac{r}{K\alpha}(S_0 - C_0(\tilde{r}_c))$ (for derivation, see Appendix (VII C 3)). This condition signals the presence of an unstable positive interior equilibrium when $\mathcal{R}_0^C < 1$, but sufficiently close to one, which will intersect with the infection-free equilibrium $\mathcal{E}_0$ at $\mathcal{R}_0^C = 1$, exchange stability and become negative when $\mathcal{R}_0^C > 1$. This type of bifurcation is known as a *backward* bifurcation. The unstable positive equilibrium

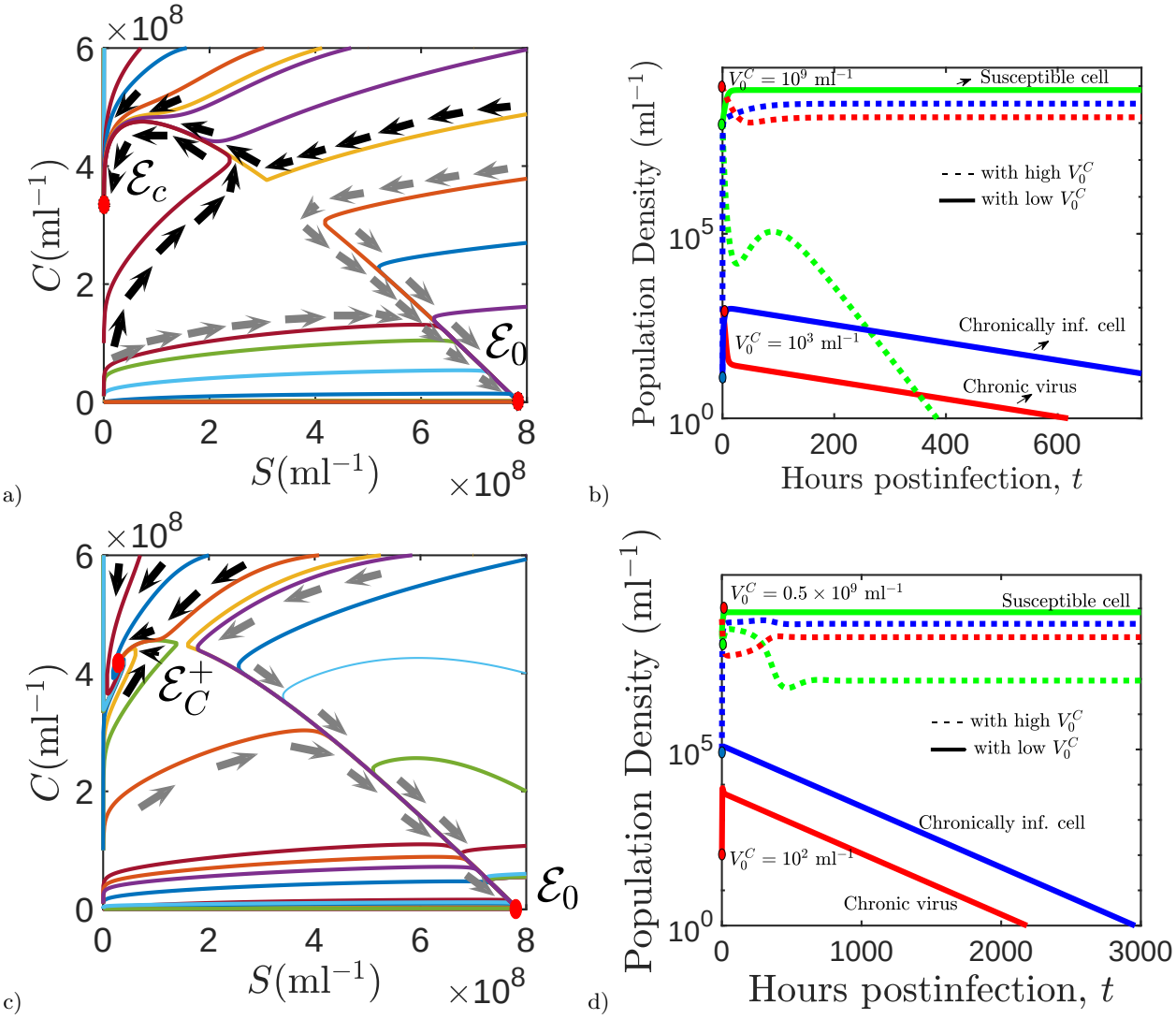

FIG. 2: *Bistable dynamics displayed by chronic-only system (III).* a) Phase plane of the system (III), where bistability occurs with local stable chronic-only equilibrium $\mathcal{E}_c = (0, C_0, V_c)$ and infection-free equilibrium $\mathcal{E}_0 = (S_0, 0, 0)$. b) Corresponding time dependent solutions of the system (III). Chronically infected cells competitively exclude the susceptible cells when the initial chronic virus density, V_0^C, is high or vice versa for low initial virus density size V_0^C. The parameter values are identical to the ones in Table I, except $\tilde{\phi} = 1.5 \times 10^{-9}$ ml/hr, $\tilde{r} = 0.08$ hrs $^{-1}$, $\alpha = 1/27$. The initial virus and host densities are $S_0 = 10^8$ viruses/ml, $C_0 = 10$ hosts/ml, $V_0^C = 10^3$ hosts/ml (low density) and $V_C(0) = 10^9$ hosts/ml (high density). c) Phase plane of the system (III), where bistability occurs with infection free equilibrium $\mathcal{E}_0$ and positive equilibrium $\mathcal{E}_C^+ = (S_C^+, C_C^+, V_C^+)$, where susceptible and chronically infected cells coexist. d) Corresponding time dependent solutions of the system (III). Bistability occurs with positive equilibrium (with high V_0^C) and infection free equilibrium (with low V_0^C). The parameter values are identical to the ones in part (a)-(b), except $\tilde{\phi} = 10^{-9}$ ml/hr. The initial virus and host densities are $S_0 = 2 \times 10^8$ viruses/ml, $C_0 = 10^5$ hosts/ml, $V_0^C = 10^2$ hosts/ml (low density) and $V_0^C = 5 \times 10^(8)$ hosts/ml (high density).

(when $\mathcal{R}_0^C < 1$), which satisfies one of the equations (6), forms part of a separatix, separating basins of attraction of distinct attractors. One of the attractors is $\mathcal{E}_0$, since $\mathcal{R}_0^C < 1$ is the condition for local stability. Interestingly, the other attractor can vary depending on parameter region, as model (**??**) displays multiple types of bistable dynamics.

One form of bistability in model (**??**) occurs when both the infection-free equilibrium $\mathcal{E}_0$ and the chronic-only equilibrium $\mathcal{E}_c$ are locally stable, and thus are both attractors. The condition for local asymptotic stability of $\mathcal{E}_c$ (Theorem VII.3 in Appendix (VII C 1)) is given by

$$\frac{S_0}{C_0} - 1 < \frac{k\tilde{\phi}\alpha}{r\mu}. \tag{9}$$

Thus, if this condition holds, when $\mathcal{R}_0^C < 1$, then the fates of the chronic and susceptible host populations

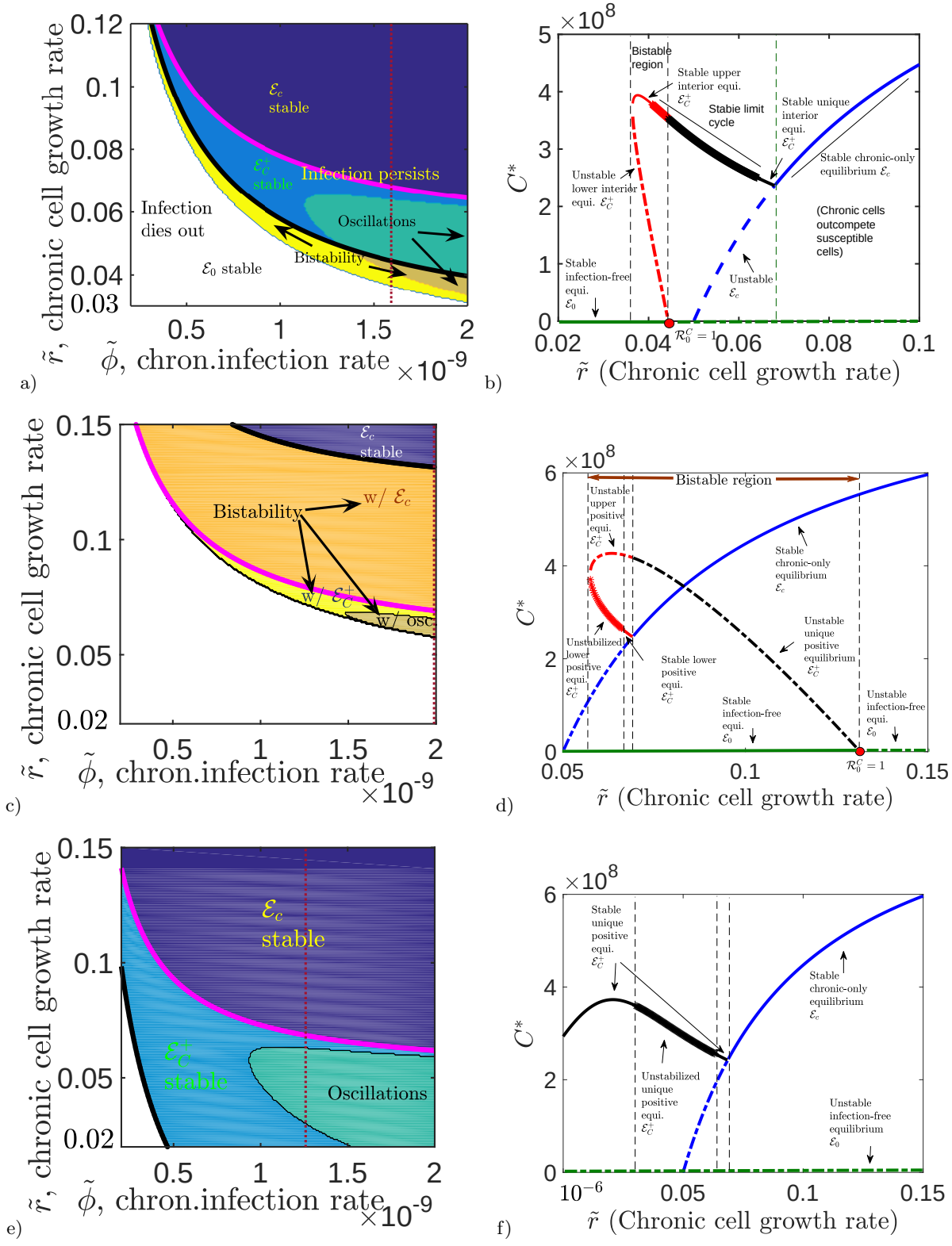

FIG. 3: a)Distinct chronic infection regimes ($\alpha = 1/21$) b) Corresponding bifurcation diagram of the chronic subsystem (displayed in the parameter region part (a)) when $\tilde{\phi} = 1.6 \times 10^{-9}$ (See the vertical dashed red line). c) Distinct chronic infection regimes when $\alpha = 1/28$, (d) Corresponding bifurcation diagram when $\tilde{\phi} = 2 \times 10^{-9}$. e) Distinct chronic infection regimes when $\alpha = 1/17$, f) Corresponding bifurcation diagram when $\tilde{\phi} = 1.25 \times 10^{-9}$. The rest of the parameter values are identical to the ones in Table I.

depends on the initial size of chronically infected host-virus concentration as shown in Figure (2)(a)-(b).

TABLE I: Lytic & Chronic Equilibria & Stability Conditions

Equi. (*Lytic*-$\mathcal{E}^*$)	S^*	I^*	V^*	Stability conditions
$\mathcal{E}_0^0$	0	0	0	$r < d$
$\mathcal{E}_0$	S_0	0	0	$\mathcal{R}_0^L < 1$
$\mathcal{E}_L^+$ (*)	S_L^+	I_L^+	V_L^+	See [1]
Equi. (*Chronic*-$\mathcal{E}^*$)	S^*	C^*	V^*	Stability conditions
$\mathcal{E}_0^0$	0	0	0	$r < d$
$\mathcal{E}_0$	S_0	0	0	$\mathcal{R}_0^L < 1$
$\mathcal{E}_c$	0	C_0	V_c	$\frac{S_0}{C_c^*} - 1 < \frac{k\tilde{\phi}\alpha}{r\mu}$
$\mathcal{E}_{C,i}^+$ (*),(**)	$S_{C,i}^+$	$C_{C,i}^+$	$V_{C,i}^+$	See Section (VII C 4)

(*) It can undergo *Hopf bifurcation*.

(**) Existence of one or both of these positive interior equilibria when $\mathcal{R}_0^C < 1$ indicates bistability.

In this case, if the initial virus or chronically infected cell concentration is low, then the virus goes extinct; however, for large enough initial concentrations, the system converges to the equilibrium state, $\mathcal{E}_c$, where only chronically infected cells survive. The biological intuition is that for certain parameter regimes, higher chronically infected cell densities allow the chronically infected cells to outcompete susceptible cells. So in an environment, where chronic cell/virus density is large, even if $\mathcal{R}_0^C < 1$, virus can change the fate of the cell population in such a way that chronically infected cells are sustained. The Fig. 3(c) shows the parameter region where this type of bistable dynamics occurs. The corresponding region in the bifurcation diagram, Fig. 3(d), shows that in addition to the stable infection-free equilibrium, $\mathcal{E}_0$, and stable chronic-only equilibrium, $\mathcal{E}_c$, there is one unstable positive equilibrium $\mathcal{E}_C^+$ (in certain cases there can be two unstable interior equilibria; see Fig. 12(h) in Appendix).

The other type of bistability consists of the infection-free equilibrium $\mathcal{E}_0$ and a positive interior coexistence equilibrium, $\mathcal{E}_{C,i}^+$, given by (7)) or a positive periodic solution as attractors. Fig. 2(c) depicts the phase plane diagram of this scenario. The corresponding time-dependent solutions of model variables $S(t), C(t)$, and $V_C(t)$ are shown in Fig.2(d) for multiple initial conditions (S_0, C_0, V_0^C). These figures show that larger initial chronic virus concentration V_0^C results in coexistence of chronic and susceptible cells, yet when the initial chronic virus concentration, V_0^C, is small, susceptible cells competitively exclude the chronic cell population.

To study the local stability of the positive interior equilibrium, $\mathcal{E}_+$, we evaluate the Jacobian Matrix around this equilibrium and study the sign of the real part of the eigenvalues, which are the roots of the characteristic equation derived from the Jacobian Matrix (see Appendix VII C 4). Analytical and numerical results suggest that the positive interior equilibrium can lose its stability via Hopf Bifurcation. For example, Fig. 9 in Appendix VII C 4, shows the interval of $\tilde{r}$, on which the sign of the complex eigenvalues switch its sign from negative (the case $\mathcal{E}_C^+$ is locally stable) to positive ($\mathcal{E}_C^+$ is unstable) or vice-versa. At the critical point, where the real part of the complex eigenvalues become zero, the equilibrium $\mathcal{E}_C^+$ undergoes Hopf bifurcation. We obtain Hopf bifurcation in Fig. 3(b)-(d)-(e) in different settings. In Fig. 3(a), the stable "upper" interior equilibrium undergoes Hopf Bifurcation at a critical value of $\tilde{r}$ in bistable setting (when $\mathcal{R}_0^C < 1$). In Fig.3 (a), the system also displays Hopf bifurcation when $\mathcal{R}_0^C > 1$ as the unique interior equilibrium stabilizes and limit cycle ceases to exist. Other parameter regimes where Hopf bifurcation of an interior equilibrium occurs are displayed in Fig.3 (d) and (f), including the case where the "lower" interior equilibrium undergoes the Hopf bifurcation.

In certain parameter regions, the chronic-only equilibrium appears to be globally stable. This occurs when $\mathcal{R}_0^C > 1$ and the chronic-only equilibrium $\mathcal{E}_c$ becomes locally stable (condition given by (9)). Here, a transcritical bifurcation occurs in which the stable interior equilibrium intersects with $\mathcal{E}_c$, exchanging stability and becoming negative through the boundary $S = 0$. This type of bifurcation, along with the others mentioned earlier, are all observed in Fig. 3(b)-(d), where when varying $\tilde{r}$, the chronic subsystem exhibits

- *Saddle-node* bifurcation, where at a critical value of $\tilde{r}$, the bifurcation diagram branch out two equilibria with one stable equilibrium and one unstable equilibrium.
- *Transcritical* bifurcation, where at a critical value of $\tilde{r}$, the stability of two equilibria with one stable and one unstable equilibrium, switches as they pass through at this critical point.
- *Backward* bifurcation, where as $\tilde{r}$ increases toward the critical $\tilde{r}_c$ (with $\mathcal{R}_0^C(\tilde{r}_c) = 1$), then the system exhibits an unstable positive equilibrium along with the stable infection-free equilibrium. It is also a transcritical bifurcation.
- *Hopf* bifurcation, where as $\tilde{r}$ increases (or decreases) the stable interior equilibrium loses its stability at a critical point and displays sustained oscillations.

Distinct bifurcation dynamics displayed by the chronic subsystem (III) are undoubtedly very interesting. We remark that there are even further distinct stability scenarios for equilibria, although they have similar qualitative dynamics to some of the cases described throughout

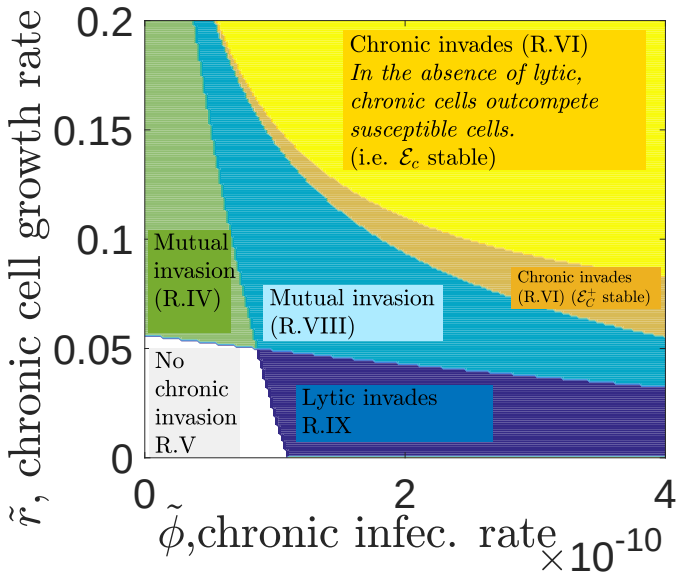

FIG. 4: *Infection, invasion and mutual invasion parameter regimes of chronically & lytic infecting viruses.* On the x-axis, we vary the chronic infection rate, $\tilde{\phi}$, and on the y-axis, we vary chronic cell growth rate, $\tilde{r}$. Given the lytic parameter values on this map, we have $\mathcal{R}_0^L > 1$. The contour map displays in what parameter regime chronically (lytic) infecting virus invade lytic (chronic) virus population and when it fails to do so. Mutual invasion regimes provide the coexistence region. The parameter values are identical to the ones in Table I. The analytical conditions, providing these regimes, are given in Table IV.

this section (see Appendix). The different bifurcations depict how the nature of chronic infection mode can significantly change the interactions and population dynamics of viruses and their hosts (see Fig.11). As seen in Fig. 3, the varying magnitude of the chronic cell growth rate, $\tilde{r}$, and chronic infection rate,$\tilde{\phi}$, can result in many distinct complex population dynamics outcomes, resulting in significant change in the abundance and the dynamics of host cells and their viruses.

IV. MULTI-STRAIN MODEL: INVASION DYNAMICS

Next, we move to the full multi-strain model (I) in order to investigate *how interaction of lytic and chronic viruses with a common microbial host can result in distinct ecological outcomes.* Competition between two species or population variants results in competitive exclusion or coexistence. Two species often cannot occupy the same niche, with the more fit species driving the other to extinction. However, heterogeneous strategies can allow for two species to both exploit a common resource and coexistence becomes a possible outcome. The starting point for analyzing competition between two species is to determine *when each species can establish their population in the presence of the other resident species.* In this section, we study under what conditions the lytic (chronic) virus type can successfully invade a resident chronic (lytic) virus population.

First, we formulate invasion fitness quantities of both virus types. An *invasion fitness quantity* is a threshold value, allowing to predict, in theoretical framework, whether a virus type can invade a distinct resident virus population.

Assuming that by the time at which lytic virus is introduced, the resident chronic virus population is at its equilibrium $\mathcal{E}_+^\dagger = (S_C^+, 0, 0, C_C^+, V_C^+)$, where positive components are given by (7), we obtain the lytic invasion fitness quantity $\mathcal{R}_{inv}^L$ as follows:

$$\mathcal{R}_{inv}^L = \frac{\beta\eta}{\eta + d}\frac{\phi S_C^+}{\phi S_C^+ + \mu}$$

It can be interpreted as the reproduction number of lytic cells at the boundary equilibrium $\mathcal{E}_+^\dagger$, analogous to the basic reproduction number $\mathcal{R}_0^L$, which is calculated at the infection-free equilibrium $\mathcal{E}_0$ instead.

Analytical results suggest that a subpopulation of lytic viruses invade chronic resident population (when it is at its equilibrium $\mathcal{E}_+^\dagger = (S_C^+, 0, 0, C_C^+, V_C^+)$ if and only if $\mathcal{R}_{inv}^L > 1$, i.e. the boundary chronic infection equilibrium is unstable with respect to invasion (see Appendix VII D). If $\mathcal{R}_{inv}^L < 1$, then the boundary chronic infection equilibrium is locally asymptotically stable, considering the parameter region where Hopf bifurcation does not occur. Note that in the region where the resident chronic population is already oscillating (at a stable limit cycle) upon arrival of lytic viruses, then the invasion depends on

a linear periodic system (given by the Next-Generation matrix at the limit cycle).

We can also formulate the threshold quantity providing whether chronic cells or viruses can invade the resident lytic population, when at the equilibrium $\mathcal{E}_L^+ = (S_L^+, I_L^+, V_L^+, 0, 0)$, where positive components are given by (2). The *chronic invasion fitness quantity*, $\mathcal{R}_{inv}^C$, is defined as

$$\mathcal{R}_{inv}^C = \frac{\tilde{r}}{\tilde{d}}(1 - \frac{N_L^+}{K}) + \frac{\tilde{\phi} S_L^+}{\tilde{\phi} S_L^+ + \mu} \frac{\alpha}{\tilde{d}},$$

where $N_L^+ = S_L^+ + I_L^+$. When a resident lytic type is at its equilibrium $\mathcal{E}_L^+ = (S_L^+, I_L^+, V_L^+, 0, 0)$, rare (a small initial density of) chronically infecting viruses can only invade if $\mathcal{R}_{inv}^C > 1$. Otherwise if $\mathcal{R}_{inv}^C < 1$, analogous conclusions hold as in the case of lytic invading chronic.

Having both invasion threshold quantities, $\mathcal{R}_{inv}^i$, along with basic reproduction numbers, $\mathcal{R}_0^i$, where $i \in \{L, C\}$, we can study distinct under what conditions invasion of one type or infection take place. Table IV in Appendix gives distinct cell and virus fates under distinct values of these invasion and infection thresholds when the initial chronic virus or cell density is sufficiently low. Fig.4 shows distinct parameter regimes where outcomes of interactions varies such that chronic virus can substitute the lytic viruses (R.VI), while fails to invade in another region (R.IX). Chronic invasion can also result in coexistence (R.IV & R.VIII) and exclusion of both types (R.V), which will be further discussed in the next section.

V. COMPETITION & COEXISTENCE OF LYTIC AND CHRONIC VIRUSES

A. Heterogeneous viral strategies promote coexistence

The multi-strain system (I) can have a unique coexistence equilibrium $\overline{\mathcal{E}}^\dagger = (S^\dagger, I^\dagger, V_L^\dagger, C^\dagger, V_C^\dagger)$, derived as

$$\begin{aligned}
S^\dagger &= \frac{\mu(d+\eta)}{\phi(\beta\eta - (d+\eta))}, \\
I^\dagger &= \frac{\left(\frac{K}{\tilde{r}}\left[\frac{\tilde{\phi}\alpha S^\dagger}{\tilde{\phi} S^\dagger + \mu}\right] + C_0\right) - (S^\dagger + A(S^\dagger))}{(1 - B(S^\dagger))}, \\
V_L^\dagger &= \frac{(d+\eta) I^\dagger}{\phi S^\dagger}, \\
C^\dagger &= A(S^\dagger) - I^\dagger B(S^\dagger), \\
V_C^\dagger &= \frac{\alpha C^\dagger}{\tilde{\phi} S^\dagger + \mu},
\end{aligned}$$

where

$$\begin{aligned}
A(S^\dagger) &= \frac{(S_0 - S^\dagger)}{W(S^\dagger)}, \\
B(S^\dagger) &= \frac{\frac{K(d+\eta)}{r S^\dagger} + 1}{W(S^\dagger)},
\end{aligned}$$

with

$$W(S^\dagger) = 1 + \frac{K}{r} \frac{\tilde{\phi}\alpha}{\tilde{\phi} S^\dagger + \mu}.$$

(see Appendix VII E). The expressions for $\overline{\mathcal{E}}^\dagger$ are too complicated in order to analytically determine the conditions for its positivity. However, numerical results show that equilibrium $\overline{\mathcal{E}}^\dagger$ can be positive in certain parameter regions, in particular when both invasion conditions $\mathcal{R}_{inv}^i, i \in \{L, C\}$ are greater than one (discussed further below). Therefore, the system can have a unique coexistence equilibrium for certain parameter regimes. In Figure (13), solutions tend to this coexistence equilibrium asymptotically. The coexistence equilibrium $\mathcal{E}^\dagger$ can lose its stability via Hopf bifurcation, in which case both virus densities oscillate and converge to a limit cycle as shown in Figure 13(d).

There are parameter regions where both invasion conditions $\mathcal{R}_{inv}^i, i \in \{L, C\}$ are greater than one, which suggests persistence of both lytic and chronic virus for these parameters. There are two distinct scenarios where $\mathcal{R}_{inv}^i > 1, i \in \{L, C\}$ as shown in Table IV. In particular, Region IV depicts an interesting scenario where $\mathcal{R}_0^C < 1$ but $\mathcal{R}_{inv}^i > 1, i \in \{L, C\}$, so that chronic can be wiped out in the absence of lytic virus, yet both viruses persist together in the multi-strain model (this scenario is discussed further in Section V B). The other case of coexistence is where all thresholds $\mathcal{R}_0^i, \mathcal{R}_{inv}^i$ are greater than one (see Fig. 4).

In either case of coexistence, the heterogeneity of the viral strategies is critical for the persistence of both virus strains. Indeed if $\tilde{r} = 0$, i.e. the chronic virus only reproduces through standard viral replication (budding or bursting of infected cells, as in the case of lytic virus), then there is no coexistence equilibrium except in the case $\mathcal{R}_0^L = \mathcal{R}_0^C$. In addition, when $\tilde{r} = 0$, the invasion fitness quantities reduce to $\mathcal{R}_{inv}^i = \frac{R_0^i}{R_0^j}$, $i \neq j$ (shown in Appendix VII.9); thus it is not possible for both invasion conditions to be greater than one. Therefore, in our study coexistence of the two virus types hinges upon the additional replication technique displayed by the chronic virus; namely being long-lived and passing on to the microbial host daughter cells after cell division.

TABLE II: Multi-strain Equilibria & Stability Conditions

Multi-strain-$\overline{\mathcal{E}}$	$S^\dagger$	$I^\dagger$	$V_I^\dagger$	$C^\dagger$	$V_C^\dagger$	Stability conditions
$\overline{\mathcal{E}}_0^0$	0	0	0	0	0	$r < d$
$\overline{\mathcal{E}}_0$	S_0	0	0	0	0	$\mathcal{R}_0^i < 1$, $i \in \{L, C\}$
$\overline{\mathcal{E}}_L^+$ (*)	S_L^+	I_L^+	V_L^+	0	0	$\mathcal{E}_L^+$ stable, & $\mathcal{R}_{inv}^C < 1$
$\overline{\mathcal{E}}_c$	0	0	0	C_0	V_c	$\mathcal{E}_c$ stable
$\overline{\mathcal{E}}_{C,i}^+$ (*),(**)	$S_{C,i}^+$	0	0	$C_{C,i}^+$	$V_{C,i}^+$	$\mathcal{E}_{C,i}^+$ stable, & $\mathcal{R}_{inv}^L < 1$
$\overline{\mathcal{E}}^\dagger$ (*)	$S^\dagger$	$I^\dagger$	$V_I^\dagger$	$C^\dagger$	$V_C^\dagger$	See Section (VII E 2)

(*) It can undergo *Hopf bifurcation*.

(**) Existence of one or both of these positive interior equilibria when $\mathcal{R}_0^C < 1$ indicates bistability.

B. Lytic Virus Facilitates Persistence of Chronic Virus

Lytic infection can alter the dynamics between the distinct reproducing cell types (chronic and susceptible) by reducing cell competition through lysing susceptible cells, thereby facilitating the persistence of chronically infected cells. However this potential (indirect) beneficial interaction goes in conflict with the competition between virus types for common microbial hosts.

How the lytic and chronic virus interactions modulate the biodiversity of the virus-microbe system depends on the parameter regimes upon which the fitness quantities change. A dramatic instance of lytic virus benefiting chronic virus is in the regime IV, where the chronic virus requires the lytic virus for survival and invasion. For this case, the chronic virus population will not become established in the absence of lytic virus, yet if lytic virus is present in the system, then the chronic virus will persist. The biological reasoning behind this unexpected result is the following: In a wholly susceptible population without lytic virus, chronically infecting cells face higher cell competition due to larger total microbial cell density, whereas if lytic virulent viruses are present, the amount of cells is decreased through lysis, reducing cell competition, which increases net reproduction of chronically infected cells, allowing for chronic invasion. Indeed, analytically we observe that a virulent lytic virus type reduces total cell population $N_L^+ = S_L^+ + I_L^+$, which increases the average chronic offsprings produced, $\frac{\tilde{r}}{\tilde{d}}(1 - \frac{N_L^+}{K})$, above what it would be in the absence of infection. In particular, for parameter values in regime IV, we obtain $\mathcal{R}_{inv}^C > 1 > \mathcal{R}_0^C$ (see Fig.4b).

We also notice that this beneficial interaction only goes one way as lytic infection can not be "rescued" by chronic viruses. Lytic viruses are more apt to persist without chronic infection since they can access a larger amount of susceptible cells (higher $\mathcal{R}_0^L$), and there is no reverse effect of cell competition on their growth. Analytically, we see that

$$\mathcal{R}_0^L = \frac{\beta\eta}{\eta + d}\frac{\phi S_0}{\phi S_0 + \mu} > \frac{\beta\eta}{\eta + d}\frac{\phi S_C^+}{\phi S_C^+ + \mu} = \mathcal{R}_{inv}^L$$

since S_0 is always greater than S_C^+.

It is *interesting* that in the regime IV, chronically infected cells not only are rescued from extinction by the lytic virus, the chronically infected population can persist at the top of the cell abundance hierarchy (infected or susceptible). Indeed, observe Fig.13, where we show how the final size of abundance of susceptible, chronically and lytic infected host population at their equilibrium changes with varying lysis rate, η. If lytic virus were removed from the system or become extinct due to sensitivity to stochastic fluctuations, susceptible cells replenish again and as a result of host competition, the chronically infected cells would face extinction again. So chronically infected cells benefit from the mutual relationship with lytic virus. This coexistence mechanism which favors survival and large chronically infecting virus abundance may explain both the observed virus diversity and relative higher prevalence of temperate virus often found in nature []. Note that temperate viruses can be modeled similar to chronic viruses in system (**??**), with additional terms describing probability of transition from lysogenic to lytic which can disappear assuming the fast rate of lysis (quasi-steady state assumption).

This study also opens another question: how will lytic virus virulence, here measured by the lysis rate η, evolve? In virus-microbe systems, increasing virulence (η) decreases the life span of infected microbial hosts ($1/\eta$), which may in return decrease the amount of virus particles releases during lysis because of physiological limits, but here we assume the burst size β remains constant. Our results suggest that the evolution of virulence of lytic viruses can be influenced by the competing chronic virus species. Numerically and analytically, we observe that lytic virus abundance drastically decreases upon the lysis rate η increasing past the critical value where chronically infection virus invade and coexist (see Fig.7a). Conversely, less virulent virus can draw the chronic virus to the extinction. Thus in an environment, where susceptible cells can sustain themselves in high abundance, the lytic virus might evolve toward being less virulent for the sake of outcompeting the chronic virus population and persisting at much higher abundance. Evolution of lytic virus toward less virulence may be another underlying reason behind the recent observations of larger abundance of temperate virus in nature [**?**]. The more rigorous argument can be done by studying ESS (Evolutionary stable strategies), in this model or an extended version with mixed strategies, i.e. one type virus display both type infection modes, which will be the next future work.

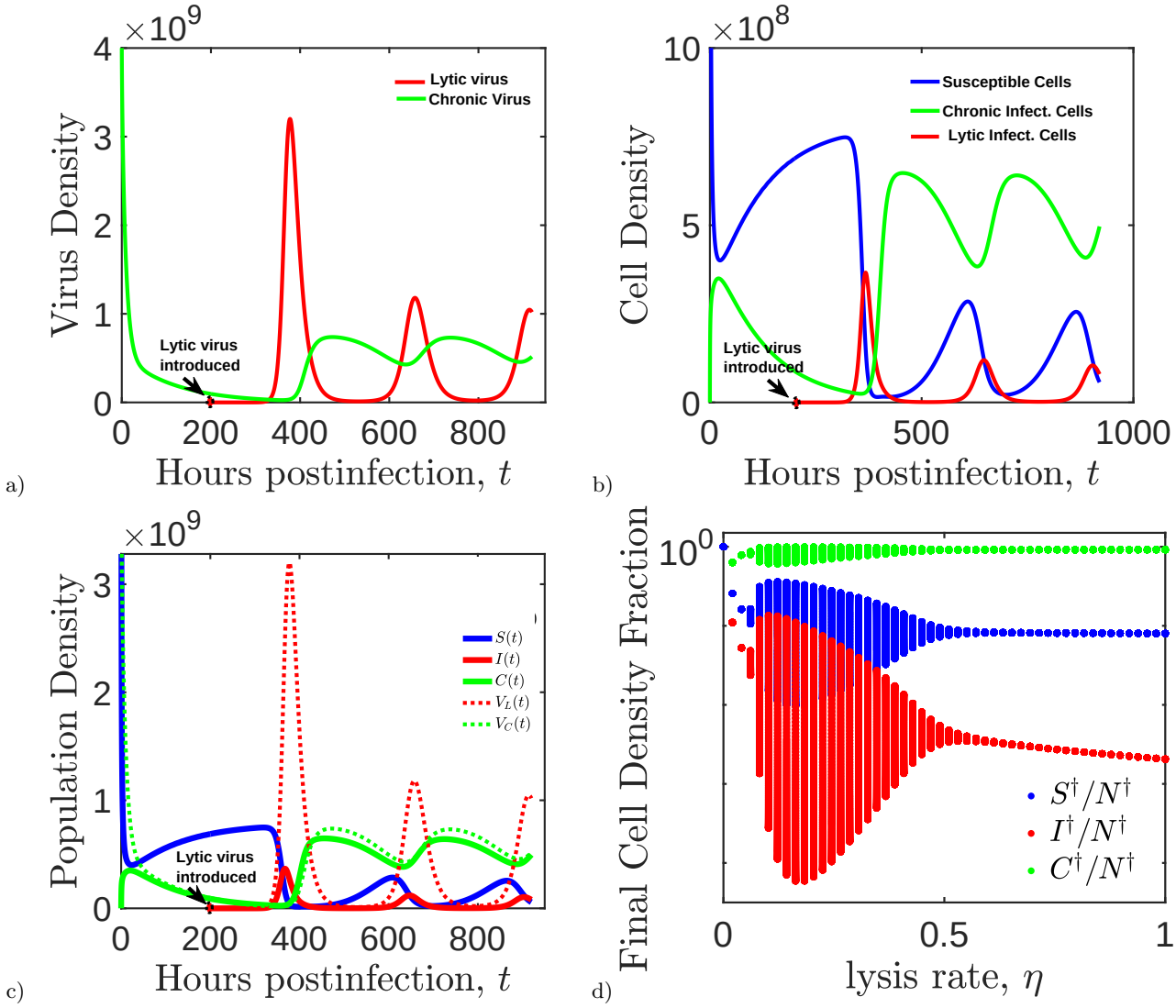

FIG. 5: a) "Rescue" of chronically infecting viruses by lytic viruses ($\eta = 0.0526$). b)Changing microbial host cell population dynamics after lytic virus introduction. b)Microbial host-virus population dynamics before and after introduction of lytic viruses. The initial virus and host densities are $S_0 = 10^10$ viruses/ml, $V_0^C = 0.04 \times S_0$ hosts/ml, $C_0 = I_0 = V_0^L = 0$ hosts/ml. d) Fraction of asymptotic cell density with respect to virulence rate η. The solid vertical lines display the sustained limit cycles with their magnitudes. The parameter values are identical to the ones in Table I.

VI. CONCLUSIONS

There are many ways microbes and their viruses interact and display distinct adaptations, infection modes and life cycles. The ability to make predictions on the microbial host and virus evolutionary strategies requires an understanding of their interactions in nature and the influence of these interactions on their abundance and fitness. In this study, we model distinct viral infection strategies (lytic & chronic) exploiting a microbial host population and find the following:

i) Chronic virus infection significantly affects the microbial host ecology and can induce more complex dynamics than lytic infection.

ii) In an environment where lytic and chronic viruses compete, the heterogeneity in their infection modes promotes the coexistence of the two virus species, and the presence of lytic virus can benefit chronic virus, even causing the persistence of chronic infection.

iii) Higher virulence of lytic viruses can be more beneficial for persistence chronic infection, which in turn can be detrimental for the lytic virus abundance. Thus our hypothesis is that this may lead lytic viruses to evolve toward less virulence. (In a model allowing for mixed viral strategies, this may manifest as evolution of an intermediate level of lysis or evolution of dimorphism).

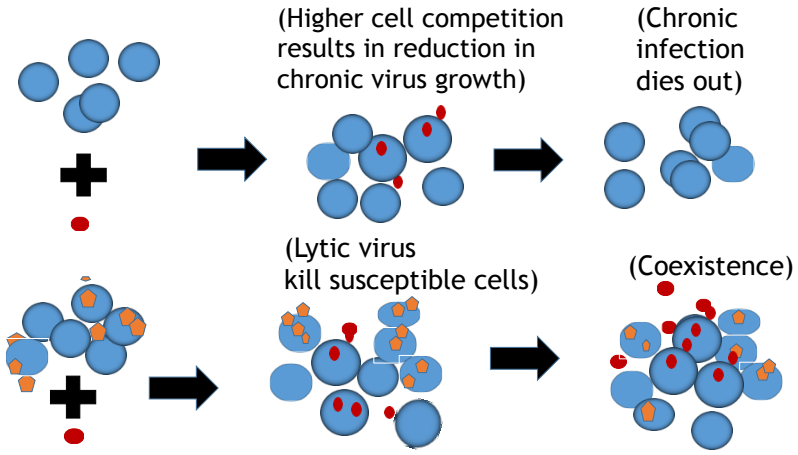

FIG. 6: Schematic representation of the outcome of interactions when a rare chronic virus introduced to a wholly susceptible cell population (upper) or when introduced to a lytic infected population (down). The chronic infection can persist only when lytic infection is already established among the susceptible host population.

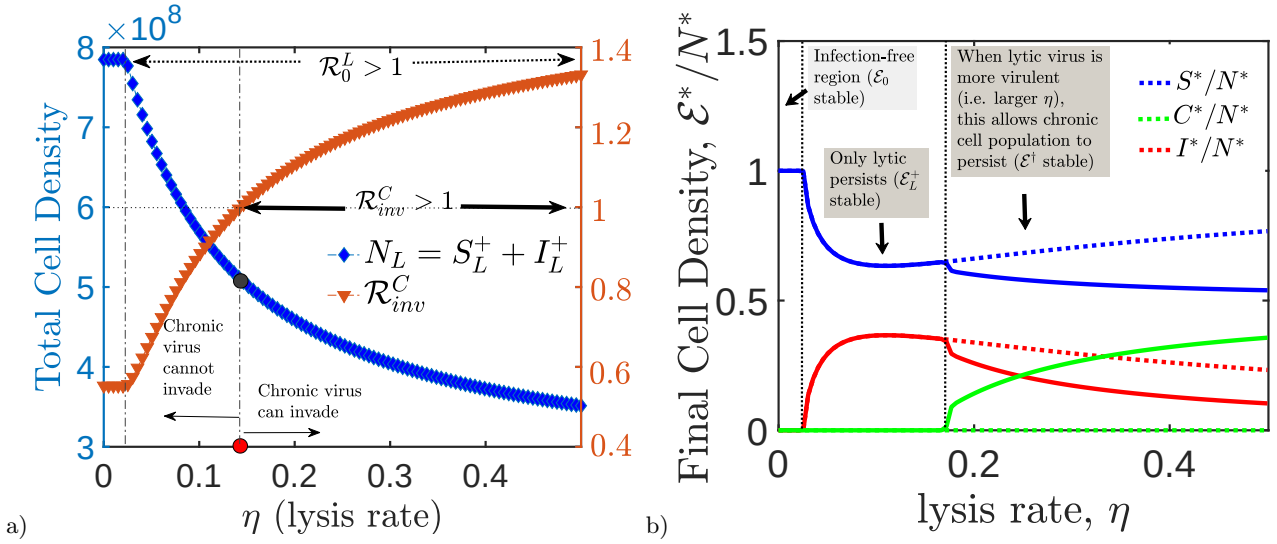

FIG. 7: a) *Invasiveness of chronic virus vs. lytic virus virulence.* As lytic virus become more virulent, it decreases the total cell density, $N_L^+ = S_L^+ + I_L^+$, at the equilibrium and increases the invasion fitness, $\mathcal{R}_{inv}^C$, of chronic virus. If $\mathcal{R}_{inv}^C > 1$, chronic can invade the lytic resident population; otherwise, if $\mathcal{R}_{inv}^C < 1$ it dies out. b) *The final cell density fraction with respect to varying lysis rate* η. The dashed line represents the fraction of lytic and susceptible cell densities at steady state in the absence of chronic infection. The solid lines display the fraction of cells densities at equilibrium and the persistence of chronic infection when lytic virulence, η, is larger. The parameter values are identical to the ones in Table I, except $\tilde{r} = 0.1$, $\phi = 0.25 \times 10^{-10}$ and $\beta = 15$.

We observe that chronic infection can affect microbial host abundance significantly. In certain parameter regions, chronic infection depicts similar dynamics to lytic infection: when $\mathcal{R}_0^i < 1$, $i \in \{L, C\}$, the virus population dies out; otherwise if $\mathcal{R}_0^i > 1$, $i \in \{L, C\}$, both virus and cell populations persists at an endemic equilibrium or at a sustained oscillation, when the positive equilibrium loses its stability via Hopf Bifurcation. Yet, the fate of chronically infecting viruses or infected hosts might also depend on the initial chronic virus density; i.e. the system presents bistable dynamics, where the initial chronic virus density changes ecological trajectories of both microbial hosts and their viruses. These bistable dynamics occurs when $\mathcal{R}_0^C < 1$, which is an interesting result in multiple dimensions: first it suggests that chronic viruses can persists even when they cannot produce one spring off averagely during their life span as opposite to lytic viruses; second bistability only occurs in the existence of chronic viruses.

More *interesting result* is the simultaneous effect of

two distinct viral infection modes on the host and virus fitness. Our analysis suggests that lytic viruses affect the cell competition in a way that, it can create a favorable environment for chronically infecting viruses, where chronically infecting virus population cannot survive in the absence of lytic viruses. Lytic viruses reduces the host competition in favor of chronically infecting cells, resulting higher chronic invasion fitness. So *lytic modulated cell competition* changes the fate of cell populations.

There are many ways by which virus can change the ecology and virulence of the other virus type (natural selection) and their microbial host cells [18]. Here we observed that in evolutionary aspect, in order to lytic viruses to increase their fitness (selective pressure), they must decrease their virulence to outcompete chronically infecting viruses. In Figure (7), we observe that there is an optimal virulence rate η_c such that at this critical point, the lytic virus outcompete the chronically infecting virus and reach at their largest abundance (higher fitness) among whole susceptible host cells; yet when it becomes more virulent, it increases the chronic virus invasion fitness. In which case, the relative abundance of lytic infected cells significantly decrease, while the abundance of chronically infected cells increases. It is interesting that while in the absence of lytic virus, chronic virus cannot survive; in the existence of it, it does not only survive, also its abundance reaches at the hierarchy of cell or virus abundance at the top with increasing lytic virulence. These can be explained by the protection induced by chronic infection and the reduction in host competition due to lytic virulence.

Despite the fact that evolution of pathogen virulence has been more often studied in epidemiological systems [38], a principle on the evolution of virulence that can extend to virus-microbial hosts systems has not been studied extensively [36, 37]. Overall, this study informs us on how lytic virus virulence can modulate virus and microbial host interactions and their fitnesses. We observe that, indeed, in virus-microbe systems, lytic virus might evolve toward less virulence to outcompete the chronic virus.

In general, viruses display both strategies (mix strategy) to explode their hosts. This study can be extended to the systems, where viruses display both strategies which allows us to study the optimal viral strategy toward maximizing its fitness. Our work clarifies the mechanism behind of the *paradoxical outcome* of competing two host species on the survival of the other type. Virus and microbial hosts interactions are highly dynamic and can give rise to coevolutionary dynamics: arm racing. To predict the host and virus evolutionary trajectories, it is important to first understand their complex interactions, individual population dynamics and the outcomes of these interactions in an ecological setting. Linking ecological dynamics and evolutionary trajectories is likely to improve our understanding of the complexity of the biological world.

VII. APPENDIX

A. Parameter Estimations

Gulbudak and Weitz [2] estimate the virus absorption rate $\phi = 2.2 \times 10^{-9}$ ml/hr from a recent experimental study of Bautista et al [11], in which the interactions takes place between the archaeon *Sulfolobus islandicus* and the dsDNA fusellovirus *Sulfulobus* spindle shaped virus (SSV9). *S. islandicus* is a globally distributed archaeon, commonly found in hot spring ecosystems. Host growth rate and carrying capacity in the absence of viruses are also estimated as $r = 0.3$ hrs^{-1} and $K = 9\times10^8$ cells/ml, respectively. Here we consider these parameters values to be $r = 0.339$ hrs^{-1}, $K = 8.947\times10^8$ cells/ml, and $\phi = 0.88 \times 10^{-10}$ ml/hr. The chronic virus absorption rate is also fixed as $\tilde{\phi} = 0.2 \times 10^{-10}$ ml/hr. The cell decay rate, d, is estimated as $d = 1/24$ hrs^{-1} in [2]. Despite the fact that the chronic infection is not virulent, it might reduce the life span of chronically infected cells due to the infection cost. Hence we fixed the value of chronic cell death rate, $\tilde{d}$ to be $1/20$ hrs^{-1}. Similarly, virus decay rate is estimated from free virus data in [11] as $\mu = 0.0866$ hrs^{-1}. In addition,Beretta and Kuang [1] estimates virus replication factor number in the range of 10 to 100 mature virus particles per day. Assuming that not all viral particles produced are infectious, we consider β to be the effective burst size and fixed as $\beta = 20$. Beretta and Kuang [1] also estimate the lysis rate, η to be $\eta = 3.3/24$ (≈ 0.138) hrs^{-1}. Here we fixed this value as $\eta = 0.33$. Although the value of chronic infection parameters, $\tilde{r}, \tilde{\phi}, \alpha$ have varied, through this study, for multiple simulations, when not varied, we chose the value of chronic cell growth rate to be $\tilde{r} = 0.2$, smaller than susceptible growth rate r, and the chronic cell virus budding off rate to be $\alpha = 1/10$. We can find *the average number of infectious viruses produced by one chronically infected cell* by multiplying the budding off rate α with cell division doubling time τ, which can be estimated by $C(t) = C(0)e^{\tilde{r}(1-\frac{S_0}{K})t}$. This estimation gives us the average number of infectious viruses produced by one chronically infected cell as $\alpha\tau \approx 2.8$.

B. Chronic Infection Dynamics Analysis

1. *Finding $\mathcal{R}_0^C$ by using Next-Generation approach*

The system has an infection-free equilibrium $\mathcal{E}_0 = (S_0, 0, 0)$ with $S_0 = K(1 - \frac{d}{r})$. Let the entries of the matrix $\mathcal{F}$ be the rates of appearance of new chronic infections, and the entries of the transition matrix $\mathcal{V}$ be the rates of transfer of individuals into or out of compartments such as death, infection, or absorption. Then the Jacobian matrix $\mathcal{J}$ evaluated at the infection-free equi-

TABLE III: Estimated parameter values of model (I)

Parameter (Host)	Fixed Value	Source	Unit
r	0.339	[2]	hrs^{-1}
K	8.947×10^8	[2]	cells/ml
d	1/24	[2]	hrs^{-1}
Parameter (Lytic)	**Fixed Value**	**Source**	**Unit**
ϕ	0.88×10^{-10}	[2]	ml/hr
β	20	[1]	
η	0.33	[1], [10]	
μ	0.0866	[2]	hrs^{-1}
Parameter (Chronic)	**Fixed Value**	**Source**	**Unit**
$\tilde{r}$	0.2	present study	hrs^{-1}
$\tilde{\phi}$	0.2×10^{-10}	[2]	ml/hr
α	1/10	present study	
$\tilde{d}$	1/20	present study	hrs^{-1}

librium $\mathcal{E}_0 = (S_0, 0, 0)$ is $\mathcal{J}_{\mathcal{E}_0} = (\mathcal{F} - \mathcal{V})|_{\mathcal{E}_0}$:

$$\mathcal{F}_{\mathcal{E}_0} = \begin{pmatrix} \tilde{r}(1 - \frac{S_0}{K}) & \tilde{\phi} S_0 \\ 0 & 0 \end{pmatrix}, \mathcal{V}_{\mathcal{E}_0} = \begin{pmatrix} \tilde{d} & 0 \\ -\alpha & (\tilde{\phi} S_0 + \mu) \end{pmatrix}$$

Then by Next Generation Matrix approach [23–25], the spectral radius of Next Generation Matrix $\mathcal{F}\mathcal{V}^{-1}|_{\mathcal{E}_0}$ gives *basic chronic reproduction number,* $\mathcal{R}_0^C$:

$$\rho(\mathcal{F}\mathcal{V}^{-1}|_{\mathcal{E}_0}) = \frac{\tilde{r}}{\tilde{d}}(1 - \frac{S_0}{K}) + \frac{\tilde{\phi} S_0}{\tilde{\phi} S_0 + \mu} \frac{\alpha}{\tilde{d}} (= \mathcal{R}_0^C), \quad (10)$$

establishing the following theorem:

Theorem VII.1 *(Local stability of $\mathcal{E}_0$) Consider the infection transmission model, given by (III). Then if $\mathcal{R}_0^C < 1$, the infection-free equilibrium, $\mathcal{E}_0$, is locally asymptotically stable, but unstable if $\mathcal{R}_0^C > 1$, where $\mathcal{R}_0^C$ is defined by (10).*

C. Preliminaries of Chronic Infection Model

To simplify the system (III), we first use the dimensionless time, $\tau = \tilde{\phi} S_0 t$, and then rescale the variables of the model (III) by letting $s = \frac{S}{S_0}, c = \frac{C}{S_0}, p = \frac{V_C}{S_0}$. Therefore we obtain the following system:

$$\begin{aligned} \frac{\mathrm{d}s}{\mathrm{d}\tau} &= as(1 - (c + s)) - sp \\ \frac{\mathrm{d}c}{\mathrm{d}\tau} &= \tilde{a}c(1 - \tilde{u}(c + s)) + sp \\ \frac{\mathrm{d}p}{\mathrm{d}\tau} &= wc - sp - mp, \end{aligned} \quad \text{(IV)}$$

where $a = \frac{r - d}{\tilde{\phi} S_0}$, $\tilde{a} = \frac{\tilde{r} - \tilde{d}}{\tilde{\phi} S_0}$, $w = \frac{\alpha}{\tilde{\phi} S_0}$, $m = \frac{\mu}{\tilde{\phi} S_0}$, $\tilde{u} = \frac{S_0}{C_0}$, with $C_0 = K(1 - \frac{\tilde{d}}{\tilde{r}})$.

1. Existence and stability of chronic-only equilibrium

Let (s^*, c^*, p^*) be the equilibrium of the system (IV). Assuming $s^* = 0$, by the equilibrium conditions, we obtain $c^* = 1/\tilde{u}, p^* = \frac{wc^*}{m}$. This establishes the following result for the original system (III):

Theorem VII.2 *The chronic subsystem (III) always has the chronic-only equilibrium $\mathcal{E}_c = (0, C_0, V_c)$, where $V_c = \frac{\alpha}{\mu} C_0$ (recall that $C_0 = K(1 - \frac{\tilde{d}}{\tilde{r}})$).*

Theorem VII.3 *The chronic-only equilibrium, $\mathcal{E}_c$, is locally asymptotically stable if and only if the condition $a(\frac{1}{c^*} - 1) < \frac{w}{m}$ holds, which is equivalent to the condition:*

$$\frac{S_0}{C_0} - 1 < \frac{K\tilde{\phi}\alpha}{r\mu}$$

for the non-dimensionalized original system (III).

Proof VII.1 *By linearizing the system (IV) around the equilibrium $\mathcal{E}_c = (0, c^*, p^*)$, we obtain the following characteristic equation:*

$$[a(1 - c^*) - p^* - \Lambda][-\tilde{u}\tilde{a}c^* - \Lambda][-m - \Lambda] = 0. \quad (11)$$

Then the Jacobian Matrix of the system (III) evaluated at $\mathcal{E}_c = (0, c^*, p^*)$, has all eigenvalues, Λ, negative if and only if the condition $a(\frac{1}{c^*} - 1) < \frac{w}{m}$ holds.

Furthermore assuming the condition above, given by (9), holds, whenever $\mathcal{R}_0^C < 1$, then the fates of the chronic and susceptible host populations depend on the initial chronically infected host and virus concentration; i.e. the system exhibits bistable dynamics. There are cases, where bistabiliy occurs with two interior equilibria (one stable and another unstable) when $\mathcal{R}_0^C < 1$. We will derive the *bistability condition* for general case in Section (VII C 3).

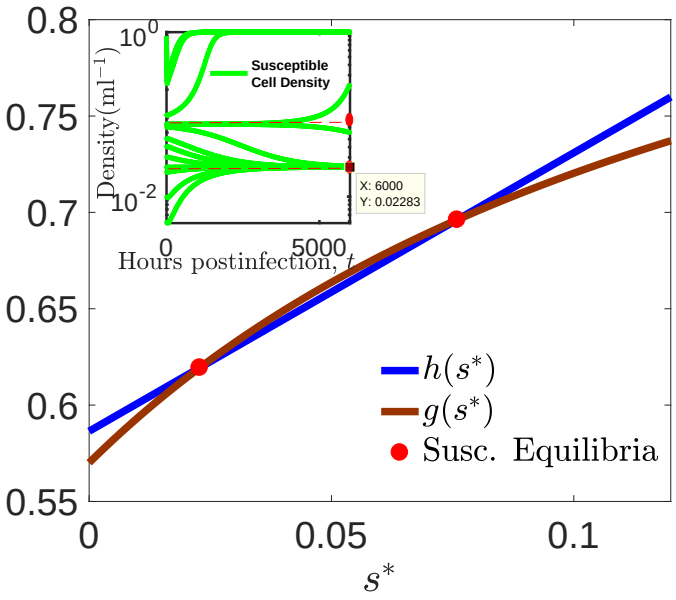

FIG. 8: *Existence of two positive interior equilibria.* The intersection of the equations $h(s^*)$ and $g(s^*)$, given in (19), provides the susceptible equilibria of the scaled system (IV). The figure above displays the case, where the system (IV) has two positive equilibria $\mathcal{E}_C^+ = (s^*, c^*, p^*)$ in positive orthant. Here the intersection of the two graphs, namely $h(s^*)$ and $g(s^*)$, in larger picture pointed with red dots. In the figure, the intersections points are $s_1^* = 0.0228$ and $s_2^* = 0.0759$ with corresponding positive equilibria $\mathcal{E}_{C,i}^+ = (s_i^*, c_i^* = s_i^*(\tilde{B} - \frac{a}{\tilde{a}\tilde{u}}) + m\tilde{B}, p_{i_2^*} = \frac{\omega c_i^*}{s_i^* + m})$. The inserted smaller figure displays time-dependent solutions of susceptible cell density with different initial conditions. The parameter values that are used here: $\tilde{r} = 1/10,\ r = 0.339,\ \tilde{d} = 1/20,\ d = 1/24,\ \alpha = 1/30,\ \tilde{\phi} = 10^{-10},\ K = 8.947 \times 10^8,\ \mu = 0.012$.

2. *Existence of Positive Equilibria*

Here, we define positive equilibrium to be the equilibrium (s^*, c^*, p^*) with all components in the positive orthant. By the equilibrium conditions, derived from the system (IV), we have

$$n^* = 1 - \frac{p^*}{a}, \tag{12}$$

$$p^* = \frac{\omega c^*}{s^* + m}. \tag{13}$$

and

$$0 = \tilde{a}c^*(1 - \tilde{u}n^*) + s^*p^*; \tag{14}$$

where $n^* = s^* + c^*$. Substituting both equations (12) and (13) into the equation (14), we get

$$c^* = s^*(\tilde{B} - \frac{a}{\tilde{a}\tilde{u}}) + m\tilde{B} \tag{15}$$

where $\tilde{B} = \dfrac{a(\tilde{u} - 1)}{\tilde{u}w}$. Then

$$n^* = s^*(\tilde{B} - \frac{a}{\tilde{a}\tilde{u}} + 1) + m\tilde{B} \tag{16}$$

By (14), we also have

$$n^* = 1 - \frac{\omega}{a}\frac{c^*}{s^* + m}. \tag{17}$$

Therefore substituting (15) into (17), we obtain

$$n^* = \frac{1}{\tilde{u}} + \frac{\omega}{\tilde{a}\tilde{u}}\frac{s^*}{(s^* + m)}. \tag{18}$$

By the equality of the equations (16) and (18), we have

$$\underbrace{s^*(\tilde{B} - \frac{a}{\tilde{a}\tilde{u}} + 1) + m\tilde{B}}_{h(s^*)} = \underbrace{\frac{1}{\tilde{u}} + \frac{\omega}{\tilde{a}\tilde{u}}\frac{s^*}{(s^* + m)}}_{g(s^*)}. \tag{19}$$

Let the left hand side of the equation be $h(s^*)$ and the right hand side of the equation be $g(s^*)$. Both functions $h(s^*), g(s^*)$ are monotone, where $h(s^*)$ is linear function with slope $(\tilde{B} - \frac{a}{\tilde{a}\tilde{u}} + 1)$ and $g(s^*)$ is an increasing saturating function of s^*, converging to $\frac{1}{\tilde{u}}(1 + \frac{w}{\tilde{a}})$ as $s^* \to \infty$. Recall that we are only considering $s^* \in (0, 1)$.

Existence and number of the positive equilibria depends on the parameter region:

- Assuming $(\tilde{B} - \frac{a}{\tilde{a}\tilde{u}} + 1) < 0$, then $h(s^*)$ is a decreasing function of s^*. In which case, if $h(0) < g(0)$, then the functions $h(s^*)$ and $g(s^*)$ do not intersect at a positive value s^*. Therefore if $h(0) < g(0)$, then the system does not have a positive equilibrium. Otherwise, if $h(0) > g(0)$, the graphs $h(s^*)$

and $g(s^*)$ intersect at a positive value, namely s_0^* in $(0,1)$, whenever $h(1) < g(1)$. In this case, the system has a positive equilibrium $\mathcal{E}_C^+ = (s^*, c^*, p^*)$ only if $s_0^*(\tilde{B} - \frac{a}{\tilde{a}\tilde{u}}) + m\tilde{B} > 0$. Notice that to obtain a positive equilibrium, we need to also obtain a corresponding positive value for $c^* = s^*(\tilde{B} - \frac{a}{\tilde{a}\tilde{u}}) + m\tilde{B}$ for the positive intersection s^*. In summary, given the condition that $(\tilde{B} - \frac{a}{\tilde{a}\tilde{u}} + 1) < 0$, the system can have at most one positive equilibrium $\mathcal{E}_+^* = (s^*, c^*, p^*)$.

- If $(\tilde{B} - \frac{a}{\tilde{a}\tilde{u}} + 1) > 0$, then $h(s^*)$ is an increasing function of s^*. Thus
  - If $h(0) < g(0)$, then h and g have one positive intersection s_0^* in (0,1) whenever $h(1) > g(1)$. In which case whenever $h(0) < g(0)$ and $h(1) > g(1)$, the system has one positive equilibrium, assuming $s_0^*(\tilde{B} - \frac{a}{\tilde{a}\tilde{u}}) + m\tilde{B} > 0$.
  - If $h(0) > g(0)$ and $h(0) \approx g(0)$, then
    - zero equilibrium when $h'(0) > g'(0)$,
    - two equilibrium when $h'(0) < g'(0)$, and $h(1) > g(1)$, assuming there is no $s^* \in (0,1) : h'(0) = g'(s^*)$.
    - or one equilibrium if $\exists s^* \in (0,1) : h'(s^*) = g'(s^*)$.
- If $(\tilde{B} - \frac{a}{\tilde{a}\tilde{u}} + 1) = 0$, then $h(s^*)$ is a constant function. Thus, if $h(0) < g(0)$, then h and g have no positive intersection point. Otherwise $h(0) > g(0)$, then h and g have at most one positive intersection point, s_0^*. Yet, to guarantee the existence of a positive equilibrium, we must have $s_0^*(\tilde{B} - \frac{a}{\tilde{a}\tilde{u}}) + m\tilde{B} > 0$. Notice that $(\tilde{B} - \frac{a}{\tilde{a}\tilde{u}}) < 0$.

In Fig.8, the graphs $h(s^*)$ and $g(s^*)$ intersect at two positive value of s^* (displayed by red dots). In the smaller inserted figure, the corresponding upper equilibrium (ordered by the size of s^*), $\mathcal{E}_{C,2}^+ = (s_2^* = 0.0759, c_2^* = 0.6202, p_2^* = 1.1512)$, is unstable and the lower equilibrium, $\mathcal{E}_{C,1}^+ = (s_1^* = 0.0228, c_1^* = 0.5966, p_1^* = 1.4420)$, is locally asymptotically stable.

By the equality of the functions $h(s^*)$ and $g(s^*)$, we can also obtain *explicit solutions* for susceptible equilibria s^* (so can do for $c^* = s^*(\tilde{B} - \frac{a}{\tilde{a}\tilde{u}}) + m\tilde{B} > 0$ and $p_2^* = \frac{\omega c^*}{s^* + m}$). Solving (19) for s^*, we obtain

$$s_{1,2}^* = \frac{-\hat{x}_2 \pm \sqrt{\hat{x}_2^2 - 4\hat{x}_1\hat{x}_3}}{2\hat{x}_1}, \tag{20}$$

where

$$\begin{aligned} \hat{x_1} &= \hat{A}_1, \\ \hat{x_2} &= \hat{A}_2 + m\hat{A}_1 - \frac{w}{\tilde{a}}, \\ \hat{x_3} &= m\hat{A}_2. \end{aligned}$$

with

$$\begin{aligned} \hat{A}_1 &= \tilde{u}\tilde{B} - \frac{a}{\tilde{a}} + \tilde{u} \\ \hat{A}_2 &= m\tilde{u}\tilde{B} - 1. \end{aligned}$$

In the original non-parametrized system (III), the equation above (20) is equivalent to

$$S_{C,i}^+ = \frac{-a_1 \pm \sqrt{a_1^2 - 4a_0a_2}}{2a_0}, \tag{21}$$

where

$$\begin{aligned} a_0 &= (B - \frac{r}{\tilde{r}} + 1)\frac{S_0}{C_0} \\ a_1 &= \frac{\mu}{\tilde{\phi}C_0}(2B - \frac{r}{\tilde{r}} + 1 + \frac{K\alpha\tilde{\phi}}{\mu\tilde{r}}) \\ a_2 &= \frac{\mu}{\tilde{\phi}S_0}(\frac{\mu}{\tilde{\phi}C_0}B - 1), \end{aligned}$$

with $B = (\frac{r}{K\alpha}(S_0 - C_0))$.

In the following subsection, we obtain the condition for backward bifurcation, proving that with vertical transmission ($\tilde{r} > 0$), the disease outcomes change significantly.

3. Bistable Dynamics

Previously, we derive local stability conditions for the infection-free equilibrium, $\mathcal{E}_0$, and chronic-only equilibrium, $\mathcal{E}_c = (0, C_0, V_c)$ and point out that when both local stability conditions hold, we obtain a bistable region. In this section, we derive a general bistability condition at a critical point ($\tilde{r} = \tilde{r}_c, C^* = 0$), with $\mathcal{R}(\tilde{r}_c) = 1$, which guarantees existence of a positive interior equilibrium, $\mathcal{E}_C^+ = (S_C^+, C_C^+, V_C^+)$ as $\tilde{r}$ increases to $\tilde{r}_c$. In which case the chronic system (III),....

Theorem VII.4 *The original non-dimensionalized system (III) has backward bifurcation at* ($\tilde{r} = \tilde{r}_c, C_C^+ = 0$) *if and only if the following conditions holds:*

$$\left(\left[B(\tilde{r}_c) - \frac{r}{\tilde{r}_c} + 1\right]\left[\frac{\mu r}{\tilde{\phi}\tilde{r}_c}\right] + \frac{\alpha K}{\tilde{r}_c} + C_0(\tilde{r}_c)\right) > 0$$

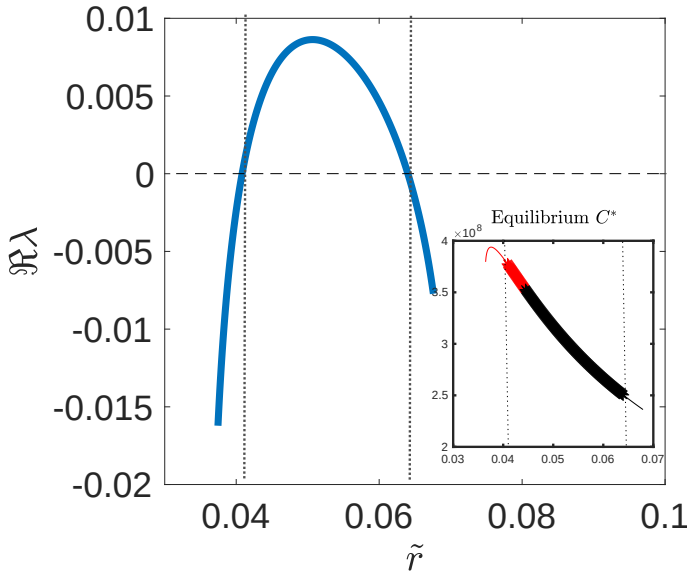

FIG. 9: *The region of Hopf bifurcation:* The larger figure displays *the real part of the complex eigenvalue*, $\Re\lambda(\tilde{r})$, v.s. chronic virus replication rate $\tilde{r}$. The smaller figure displays the chronic equilibrium C_C^+ v.s. $\tilde{r}$. In the smaller figure, we observe that as $\tilde{r}$ increases, locally stable positive equilibrium (displayed by red solid line) loses its stability and the system presents Hopf bifurcation, displaying sustained oscillation, shown with $\star$. The red color equilibrium is the upper positive equilibrium in bistability region, observed in Fig.3(b). As $\tilde{r}$ increases, the lower interior equilibrium disappear and the upper interior equilibrium become the unique positive equilibrium, displayed with black color. We obtain second Hopf bifurcation point as $\tilde{r}$ further increases. The full bifurcation diagram can be seen in Fig.3b, having the same parameter values used here.

where

$$C_0(\tilde{r}_c) = K(1 - \frac{\tilde{d}}{\tilde{r}_c}),$$

and

$$B(\tilde{r}_c) = \frac{r}{K\alpha}(S_0 - C_0(\tilde{r}_c))$$

and $\tilde{r}^c$ is a critical value of the bifurcation parameter $\tilde{r}$ such that $\mathcal{R}_0^C(\tilde{r}_c) = 1$.

Note that $\mathcal{R}_0^C(\tilde{r}_c) = 1$ if and only if $\tilde{r}_c = \dfrac{\tilde{d} - \dfrac{\alpha\tilde{\phi}S_0}{\tilde{\phi}S_0 + \mu}}{(1 - \dfrac{S_0}{K})}$.

Proof VII.2 *Recall that*

$$S_C^+ = \frac{C_C^+ - \frac{\mu}{\tilde{\phi}}B}{B - \frac{r}{\tilde{r}}} \tag{21}$$

By substituting (21) into the equilibrium condition $h(S_C^+) = g(S_C^+)$, given by (**??**)*, we get*

$$\underbrace{-C_C^+\left[\left((C_C^+ - \frac{\mu r}{\tilde{\phi}\tilde{r}})(B + 1 - \frac{r}{\tilde{r}}) - \frac{\alpha K}{\tilde{r}}\right) - \left(C_0 + (\frac{\mu B}{\tilde{\phi}})(B - \frac{r}{\tilde{r}})\right)\right]}_{F(\tilde{r}, C_C^+)}$$

$$= \frac{\mu}{\tilde{\phi}\tilde{r}}\left[B\left((\frac{\mu r}{\tilde{\phi}})[B - \frac{r}{\tilde{r}}] + \alpha K\right) + rC_0\right] \tag{21}$$

$F(\tilde{r}, C_C^+)$ is a continuously differentiable function. At the fix value $(\tilde{r} = \tilde{r}_c, C_C^+ = 0) \in \mathbb{R}^C$, where $\mathcal{R}_0^C(\tilde{r}_c) = 1$, we have

$$\frac{\partial F(\tilde{r}, C_C^+)}{\partial C_C^+}|_{(r=\tilde{r}_c, C_C^+=0)} \neq 0$$

Then by Implicit Function Theorem, there exists an open interval set $\mathcal{U}$ of $\mathbb{R}^C$ containing $\tilde{r}_c$ and such that there exists a unique continuously differentiable function, $f : \mathcal{U} \to \mathbb{R}$:

$$f(\tilde{r}_c) = C_C^+,$$

with $C_C^+ = 0$, and

$$F(\tilde{r}, f(\tilde{r}))) = \frac{\mu}{\tilde{\phi}\tilde{r}}\left[B\left((\frac{\mu r}{\tilde{\phi}})[B - \frac{r}{\tilde{r}}] + \alpha K\right) + rC_0\right]$$

for all $\tilde{r} \in \mathcal{U}$. We have an explicit expression for C_C^+ as a function of $\tilde{r}$, given by the expression of the positive equilibria $\mathcal{E}_C^+$. Implicit Function Theorem suggests that $C_C^+(\tilde{r})$ is unique and continuously differentiable w.r.t. $\tilde{r}$ in the open neighborhood of $\tilde{r}_c$, namely $\mathcal{U}$. Therefore, to see the sign of $\dfrac{\partial C_C^+}{\partial \tilde{r}}|_{(\tilde{r}=\tilde{r}_c, C_C^+=0)}$, we take implicit derivative of the equality (**??**) *w.r.t $\tilde{r}$, at the point $(\tilde{r} = \tilde{r}_c, C_C^+ = 0)$, and by doing so, we obtain*

$$(\frac{\mu r}{\tilde{\phi}\tilde{r}_c})(\frac{K\tilde{d}}{(\tilde{r}_c)^2}) + \frac{\mu}{\tilde{\phi}}\frac{r}{(\tilde{r}_c)^2}S_0 = \frac{\partial F(C_C^+)}{\partial C_C^+}\frac{dC_C^+}{d\tilde{r}}|_{(\tilde{r}=\tilde{r}_c, C_C^+=0)} \tag{22}$$

Notice that the left hand side of the equation is positive. So whenever

$$\frac{\partial F(C_C^+)}{\partial C_C^+}|_{(\tilde{r}=\tilde{r}_c, C_C^+=0)} > 0. \tag{23}$$

we obtain $\frac{dC_C^+}{d\tilde{r}}|_{C_C^+=0,\tilde{r}=\tilde{r}_c} < 0$, *implying that the system exhibits backward bifurcation at the critical point* $(\tilde{r}_c, 0)$. *Note that*

$$\begin{aligned}&\frac{\partial F(C_C^+)}{\partial C_C^+}|_{(\tilde{r}=\tilde{r}_c, C_C^+=0)}\\ &= -\left(\left[B(\tilde{r}_c) - \frac{r}{\tilde{r}_c} + 1\right]\left[\frac{\mu r}{\tilde{\phi}}\tilde{r}_c\right] + \frac{\alpha K}{\tilde{r}_c} + C_0(\tilde{r}_c)\right)\end{aligned}$$

Therefore, the system exhibits backward bifurcation at $(\tilde{r}_c, 0)$. *if and only if*

$$\left(\left[B(\tilde{r}_c) - \frac{r}{\tilde{r}_c} + 1\right]\left[\frac{\mu r}{\tilde{\phi}\tilde{r}_c}\right] + \frac{\alpha K}{\tilde{r}_c} + C_0(\tilde{r}_c)\right) > 0.$$

where

$$C_0(\tilde{r}_c) = K(1 - \frac{\tilde{d}}{\tilde{r}_c}),$$

and

$$B(\tilde{r}_c) = \frac{r}{K\alpha}(S_0 - C_0(\tilde{r}_c))$$

with

$$\tilde{r}_c = \frac{\tilde{d} - \dfrac{\alpha\tilde{\phi}S_0}{\tilde{\phi}S_0 + \mu}}{(1 - \dfrac{S_0}{K})}.$$

Remark VII.1 If the condition (8) does not hold; i.e. $\frac{\partial F(C_C^+)}{\partial C_C^+}|_{(\tilde{r}=\tilde{r}_c, C_C^+=0)} < 0$, *then the system exhibits forward bifurcation at* $(\tilde{r} = \tilde{r}_c, C_C^+ = 0)$. *Also the backward bifurcation condition* (8) *at the critical point* $(\tilde{r}_c, 0)$ *appears to be necessary and sufficient condition for the existence of two positive infection equilibria* $\mathcal{E}_C^+$.

4. *Local Stability of the Equilibria and Hopf Bifurcation (Routh-Hurwitz Criteria)*

Linearizing the system around the positive infection equilibrium $(s^*, c^* = s^*(B + \frac{a}{\tilde{a}\tilde{u}}) + mB, p^* = \frac{\omega c^*}{s^* + m})$, we obtain the following Jacobian matrix:

$$\mathcal{J}_{\mathcal{E}_C^+} = \begin{pmatrix} -as^* & -as^* & -s^* \\ -\tilde{u}\tilde{a}c^* + p^* & \tilde{a}(1 - \tilde{u}n^*) - \tilde{u}\tilde{a}c^* & s^* \\ -p^* & \omega & -(s^* + m) \end{pmatrix},$$

The characteristic equation for the Jacobian matrix $\mathcal{J}_{\epsilon_C^+} is$:

$$\lambda^3 + \hat{a}_1(s^*)\lambda^2 + \hat{a}_2(s^*)\lambda + \hat{a}_3(s^*) = 0, \tag{22}$$

where

$$\begin{aligned}\hat{a}_1(s^*) &= as^* + (s^* + m) + \tilde{a}\left(1 - \tilde{u}(2c^* + s^*)\right),\\ \hat{a}_2(s^*) &= \tilde{a}\left(1 - \tilde{u}(2c^* + s^*)\right)\left[(s^* + m) + as^*\right]\\ &\quad + as^*[(s^* + m) + (\tilde{u}\tilde{a}c^* - p^*)] + s^*(w - p^*),\\ \hat{a}_3(s^*) &= \tilde{a}\left(1 - \tilde{u}(2c^* + s^*)\right)\left[as^*(s^* + m) - s^*p^*\right]\\ &\quad + (\tilde{u}\tilde{a}c^* - p^*)[as^*(s^* + m) + s^*w] + as^*(ws^* + p^*s^*)\end{aligned}$$

with

$$\begin{aligned}c^* &= s^*(\tilde{B} - \frac{a}{\tilde{a}\tilde{u}}) + m\tilde{B},\\ p^* &= \frac{w}{s^* + m}c^*,\ s^* \in (0, 1).\end{aligned}$$

By Routh-Hurwitz Criteria, for any $s^* \in (0, 1)$, the positive equilibrium $\mathcal{E}_C^+$ is locally asymptotically stable if and only if: $\hat{a}_i(s^*) > 0$, for $i = 1, 2, 3$, and $\Delta(s^*) = \hat{a}_1(s^*)\hat{a}_2(s^*) - \hat{a}_3(s^*) > 0$. Otherwise if $\exists s_0^* \in (0, 1)$ such that $\hat{a}_1(s_0^*) > 0, \hat{a}_3(s_0^*) > 0$ and $\Delta(s_0^*) = 0$, where $\Delta(s^*)$ is a smooth function of s^*, in an open interval of s^* : $\frac{d\Delta(s^*)}{ds^*}|_{s^*=s_0^*} \neq 0$, then the system exhibits Hopf bifurcation at $s^* = s_0^*$.

The coefficients of the characteristic equation are functions of s^*, for which explicit formulas are given in (20). Because of complicated expressions of the coefficients $\hat{a}_i$, it is difficult to find any analytic condition, providing Hopf Bifurcation. Therefore we utilize numerical simulations to show that the system displays Hopf Bifurcation.

In the Fig.9, the x-axis presents the values of $\tilde{r}$ and y-axis shows how the real part of the complex eigenvalue changes w.r.t. $\tilde{r}$. The characteristic equation, given by (22), is a cubic polynomial. So the Jacobian matrix $\mathcal{J}_{\mathcal{E}_C^+}$ has either three real eigenvalues or one real and two complex conjugate eigenvalues, λ. For the case, where the Jacobian matrix $\mathcal{J}_{\mathcal{E}_C^+}$ has all eigenvalues with negative real parts, the positive equilibrium $\mathcal{E}_C^+$ is locally asymptotically stable. If the sign of the real part of the complex eigenvalues ($\Re\lambda$) changes from negative to positive as varying the bifurcation parameter $\tilde{r}$, then Hopf Bifurcation occurs at $\tilde{r} : \Re\lambda(\tilde{r}) = 0$. At the Hopf bifurcation point $\tilde{r} : \Re\lambda(\tilde{r}) = 0$, $\mathcal{E}_C^+$ lose its stability and become unstable. Hopf bifurcation occurs when the order is reversed as well: unstable $\mathcal{E}_C^+$ becomes stable. Notice that at $\tilde{r} : \Re\lambda(\tilde{r}) = 0$, we have $\Delta = 0$ while $\hat{a}_i(s^*) > 0$, for $i = 1, 2, 3$. In Fig.9, there are two parameters values $\tilde{r}$ at which Hopf Bifurcation occurs. At this points, stability of equilibrium $\mathcal{E}_C^+$ first changes from stable to unstable, and then as $\tilde{r}$ increases, it changes unstable to stable.

D. Lytic and Chronic Invasion Analysis

Assuming that when rare lytic population arrive, the chronic type (resident) is at its equilibrium

$$\overline{\mathcal{E}}_C^+ = (S_C^+, 0, 0, C_C^+, V_C^+)$$

(the expressions of positive components are given in (7)), we can estimate *the lytic invasion fitness quantity* $\mathcal{R}_{inv}^L$ by using Next Generation Matrix Approach:
Let the entries of the matrix $\mathcal{F}$ be the rates of appearance of new chronic infections among susceptible cell population in lytic infected environment, and the entries of the transition matrix $\mathcal{V}$ be the rates of transfer of individuals into or out of compartments such as death, infection, or absorption.

$$\mathcal{F}_{\overline{\mathcal{E}}_C^+} = \begin{pmatrix} 0 & \phi S_C^+ \\ 0 & 0 \end{pmatrix}, \mathcal{V}_{\mathcal{E}_0} = \begin{pmatrix} (\eta + d) & 0 \\ -\beta\eta & (\phi S_C^+ + \mu) \end{pmatrix}$$

Then the lytic invasion fitness quantity is:

$$\mathcal{R}_{inv}^L = \rho(FV^{-1}) = \frac{\phi S_C^+}{(\phi S_C^+ + \mu)} \frac{\beta\eta}{\eta + d},$$

establishing the following result:

Theorem VII.5 *The dominance equilibrium of chronic virus* $\overline{\mathcal{E}}_C^+ = (S_C^+, 0, 0, C_C^+, V_C^+)$ *is locally asymptotically stable if* $\mathcal{R}_{inv}^L < 1$ *and unstable if* $\mathcal{R}_{inv}^L > 1$.

Notice that at the chronic equilibrium $\overline{\mathcal{E}}_c = (0, 0, 0, C_0, V_c)$ (the expressions of the positive components are given in (5)), lytic invasion does not occur due to lack of susceptible cell population in the environment and the immunity provided by the chronic infection.

By similar approach, by assuming that when rare chronic population arrive, the resident lytic population is at its equilibrium

$$\overline{\mathcal{E}}_L^+ = (S_L^+, I_L^+, V_L^+, 0, 0)$$

(the expressions of positive components are given in (2)), we can also estimate *the chronic virus invasion fitness quantity* as follows:

$$\mathcal{R}_{inv}^C = \frac{\tilde{r}}{\tilde{d}}(1 - \frac{N_L^+}{K}) + \frac{\tilde{\phi} S_L^+}{\tilde{\phi} S_L^+ + \mu} \frac{\alpha}{\tilde{d}}, \text{ with } N_L^+ = S_L^+ + I_L^+,$$

establishing the following result:

Theorem VII.6 *The dominance equilibrium of lytic virus* $\overline{\mathcal{E}}_L^+ = (S_L^+, I_L^+, V_L^+, 0, 0)$ *is locally asymptotically stable if* $\mathcal{R}_{inv}^C < 1$ *and unstable if* $\mathcal{R}_{inv}^C > 1$.

E. Invasion Dynamics: Coexistence & Substitution

1. Reproduction Number of the multi-strain model

The Jacobian matrix $\mathcal{J}$ evaluated at the infection-free equilibrium $\mathcal{E}_0 = (S_0, 0, 0, 0, 0)$ is $\mathcal{J}|_{\mathcal{E}_0} = (\mathcal{F} - \mathcal{V})|_{\mathcal{E}_0}$, where

$$\mathcal{F} = \begin{pmatrix} 0 & \phi S_0 & 0 & 0 \\ 0 & 0 & 0 & 0 \\ 0 & 0 & \tilde{r}(1 - \frac{S_0}{K}) & \tilde{\phi} S_0 \\ 0 & 0 & 0 & 0 \end{pmatrix},$$

and

$$\mathcal{V}^{-1} = \begin{pmatrix} (\eta + d) & 0 & 0 & 0 \\ -\beta\eta & (\phi S_0 + \mu) & 0 & 0 \\ 0 & 0 & \tilde{d} & 0 \\ 0 & 0 & -\alpha & (\tilde{\phi} S_0 + \mu) \end{pmatrix}$$

By using the Next Generation Matrix approach for the multi-strain model, we obtain:

$$\mathcal{F}\mathcal{V}^{-1} = \begin{pmatrix} \mathcal{F}_1\mathcal{V}_1^{-1} & 0 \\ 0 & \mathcal{F}_2\mathcal{V}_2^{-1} \end{pmatrix},$$

Note that $\rho_i(\mathcal{F}_i\mathcal{V}_i^{-1}) = \mathcal{R}_0^i$. Therefore the reproduction number for the multi-strain model is

$$\mathcal{R}_0 = \max_{i \in \{L, C\}} \{\mathcal{R}_0^i\},$$

establishing the following theorem:

Theorem VII.7 *If* $\mathcal{R}_0 < 1$, *then infection-free equilibrium* $\mathcal{E}_0 = (S_0, 0, 0, 0, 0)$; *is locally asymptotically. Otherwise if* $\mathcal{R}_0 > 1$, *then* $\mathcal{E}_0$ *is unstable.*

2. Derivation of coexistence equilibrium for multi-strain model (I)

We can rearrange the multi-strain model (I) as follows:

$$\begin{aligned} \dot{S} &= \frac{rS_0}{K} S(1 - \frac{N}{S_0}) - S(\phi V_L + \tilde{\phi} V_C) \\ \dot{I} &= \phi S V_L - (\eta + d) I \\ \dot{C} &= \frac{\tilde{r} C_0}{K} C(1 - \frac{N}{C_0}) + \tilde{\phi} S V_C \\ \dot{V_L} &= \beta\eta I - (\phi S + \mu) V_L, \\ \dot{V_C} &= \alpha C - (\tilde{\phi} S + \mu) V_C, \end{aligned} \tag{21}$$

where $N = S + I + C$. An equilibrium, $\overline{\mathcal{E}}^{\dagger}(S^{\dagger}, I^{\dagger}, C^{\dagger}, V_L^{\dagger}, V_C^{\dagger})$, of the system (I) must be a solution of the system below:

$$\begin{aligned} 0 &= \frac{rS_0}{K}S^{\dagger}(1-\frac{N^{\dagger}}{S_0}) - S^{\dagger}(\phi V_L^{\dagger} + \tilde{\phi}V_C^{\dagger}) \\ 0 &= \phi S^{\dagger}V_L^{\dagger} - (\eta + d)I^{\dagger} \\ 0 &= \frac{\tilde{r}C_0}{K}C^{\dagger}(1-\frac{N^{\dagger}}{C_0}) + \tilde{\phi}S^{\dagger}V_C^{\dagger} \\ 0 &= \beta\eta I^{\dagger} - (\phi S^{\dagger} + \mu)V_L^{\dagger}, \\ 0 &= \alpha C^{\dagger} - (\tilde{\phi}S^{\dagger} + \mu)V_C^{\dagger}, \end{aligned} \tag{22}$$

By the second and fourth equations in the system (22), we have

$$V_L^{\dagger} = \frac{(d+\eta)I^{\dagger}}{\phi S^{\dagger}},\ V_L^{\dagger} = \frac{\beta\eta I^{\dagger}}{\phi S^{\dagger} + \mu} \tag{23}$$

By the equality of both equations in (23) , we obtain

$$S^{\dagger} = \frac{\mu(d+\eta)}{\phi(\beta\eta - (d+\eta))}. \tag{24}$$

By the equation fifth equation in (22), we have

$$V_C^{\dagger} = \frac{\alpha C^{\dagger}}{\tilde{\phi}S^{\dagger} + \mu}. \tag{25}$$

Substituting (25), into the third equation in (22), we get

$$N^{\dagger} = \left(\left[\frac{\tilde{\phi}S^{\dagger}\alpha}{\tilde{\phi}S^{\dagger} + \mu}\right] + \frac{\tilde{r}}{K}C_0\right)\frac{K}{\tilde{r}} \tag{26}$$

By the first equation in (22),

$$N^{\dagger} = S_0 - \frac{K}{r}\left[\frac{(d+\eta)I^{\dagger}}{S^{\dagger}} + \frac{\tilde{\phi}\alpha C^{\dagger}}{\tilde{\phi}S^{\dagger} + \mu}\right] \tag{27}$$

Substituting the equations (23) and (25) into the equation (28), we obtain

$$C^{\dagger} = A(S^{\dagger}) - I^{\dagger}B(S^{\dagger}) \tag{28}$$

where

$$\begin{aligned} A(S^{\dagger}) &= \frac{(S_0 - S^{\dagger})}{W(S^{\dagger})}, \\ B(S^{\dagger}) &= \frac{\frac{K(d+\eta)}{rS^{\dagger}} + 1}{W(S^{\dagger})}, \end{aligned}$$

with

$$W(S^{\dagger}) = 1 + \frac{K}{r}\frac{\tilde{\phi}\alpha}{\tilde{\phi}S^{\dagger} + \mu}.$$

Thus

$$N^{\dagger} = S^{\dagger} + I^{\dagger}(1 - B(S^{\dagger})) + A(S^{\dagger}). \tag{29}$$

Substituting (26) into the equation (29) and by rearranging it , we obtain

$$I^{\dagger} = \frac{\left(\frac{K}{\tilde{r}}\left[\frac{\tilde{\phi}\alpha S^{\dagger}}{\tilde{\phi}S^{\dagger} + \mu}\right] + C_0\right) - (S^{\dagger} + A(S^{\dagger}))}{(1 - B(S^{\dagger}))}. \tag{30}$$

This establishes the following result:

Theorem VII.8 *The multi-strain system (I) has at most a unique coexistence equilibrium*

$$\overline{\mathcal{E}}^{\dagger} = (S^{\dagger}, I^{\dagger}, V_L^{\dagger}, C^{\dagger}, V_C^{\dagger})$$

where

$$\begin{aligned} S^{\dagger} &= \frac{\mu(d+\eta)}{\phi(\beta\eta - (d+\eta))}, \\ I^{\dagger} &= \frac{\left(\frac{K}{\tilde{r}}\left[\frac{\tilde{\phi}\alpha S^{\dagger}}{\tilde{\phi}S^{\dagger} + \mu}\right] + C_0\right) - (S^{\dagger} + A(S^{\dagger}))}{(1 - B(S^{\dagger}))}, \\ V_L^{\dagger} &= \frac{(d+\eta)I^{\dagger}}{\phi S^{\dagger}}, \\ C^{\dagger} &= A(S^{\dagger}) - I^{\dagger}B(S^{\dagger}), \\ V_C^{\dagger} &= \frac{\alpha C^{\dagger}}{\tilde{\phi}S^{\dagger} + \mu}, \end{aligned}$$

where

$$\begin{aligned} A(S^{\dagger}) &= \frac{(S_0 - S^{\dagger})}{W(S^{\dagger})}, \\ B(S^{\dagger}) &= \frac{\frac{K(d+\eta)}{rS^{\dagger}} + 1}{W(S^{\dagger})}, \end{aligned}$$

with

$$W(S^{\dagger}) = 1 + \frac{K}{r}\frac{\tilde{\phi}\alpha}{\tilde{\phi}S^{\dagger} + \mu}.$$

Remark VII.2 Similar to the system (III)*, we also study the local stability of the coexistence equilibrium $\overline{\mathcal{E}}^{\dagger}$ for the multi-strain system* (I)*. Evaluating the Jacobian matrix around the coexistence equilibrium $\overline{\mathcal{E}}^{\dagger}$, we obtain the characteristic equation, which is a fifth degree polynomial of eigenvalue λ. The coefficients of characteristic equation can be written as functions of $S^{\dagger}$; yet due to difficult expressions of these functions, we study the local stability of $\overline{\mathcal{E}}^{\dagger}$, and the parameter regime, where the system exhibit hopf bifurcation, numerically. The Fig.13(d) depicts*

that, in the given parameter regime, the coexistence equilibrium $\overline{\mathcal{E}}^\dagger$ is locally asymptotically stable (displayed with •) for smaller value of η. Yet as η increases, at a critical value η_c, the system undergoes hopf bifurcation and displays sustained oscillations (the magnitude of the periodic solutions shown by a bar). The further increase in η restabilizes the coexistence equilibrium $\overline{\mathcal{E}}^\dagger$.

3. Competitive Exclusion when $\tilde{r} = 0$

Theorem VII.9 *Assume $\tilde{r} = 0$. If $\mathcal{R}_0^i > 1$, for $i \in \{L, C\}$, then the virus strain with largest reproduction number outcompetes the other one.*

To prove Theorem (VII.9), we will first establish the following lemma:

Lemma VII.1 *Assume $\tilde{r} = 0$. Let*

$$\hat{\mathcal{R}}_0^L := \frac{\phi S_0(\beta\eta - (\eta + d))}{\mu(\eta + d)} \text{ and } \hat{\mathcal{R}}_0^C := \frac{\tilde{\phi} S_0(\alpha - \tilde{d})}{\mu\tilde{d}}.$$

Then, for all $i \in \{L, C\}$, the reproduction numbers $\mathcal{R}_0^i$ is equivalent to $\hat{\mathcal{R}}_0^i$ for $i \in \{L, C\}$, respectively, i.e. the following conditions hold:

i. $\mathcal{R}_0^i = 1$ if and only if $\hat{\mathcal{R}}_0^i = 1$,

ii. $\mathcal{R}_0^i > 1$ if and only if $\hat{\mathcal{R}}_0^i > 1$,

iii. $\mathcal{R}_0^i < 1$ if and only if $\hat{\mathcal{R}}_0^i < 1$.

Proof VII.3

- *Case [i.] If $\tilde{r} = 0$, then*

$$\mathcal{R}_0^C = \frac{\tilde{\phi} S_0}{\tilde{\phi} S_0 + \mu} \frac{\alpha}{\tilde{d}}.$$

Therefore

$$\begin{aligned} \mathcal{R}_0^C = \hat{\mathcal{R}}_0^C &\Leftrightarrow \frac{\tilde{\phi} S_0}{\tilde{\phi} S_0 + \mu} \frac{\alpha}{\tilde{d}} = \frac{\tilde{\phi} S_0(\alpha - \tilde{d}}{\mu\tilde{d}} \\ &\Leftrightarrow (\tilde{\phi} S_0 + \mu)(\alpha - \tilde{d}) = \mu\alpha \\ &\Leftrightarrow \tilde{\phi} S_0(\alpha - \tilde{d}) = \mu\tilde{d} \\ &\Leftrightarrow \frac{\tilde{\phi} S_0(\alpha - \tilde{d})}{\mu\tilde{d}} = 1. \end{aligned}$$

- *Case [ii.]-[iii.]*

$$\begin{aligned} \mathcal{R}_0^C > 1 \ (or <) &\Leftrightarrow \frac{\tilde{\phi} S_0}{\tilde{\phi} S_0 + \mu} \frac{\alpha}{\tilde{d}} > 1 \ (or <) \\ &\Leftrightarrow \tilde{\phi} S_0(\alpha - \tilde{d}) > \mu\tilde{d} \ (or <) \\ &\Leftrightarrow \frac{\tilde{\phi} S_0(\alpha - \tilde{d}}{\mu\tilde{d}} > 1 \ (or <) \\ &\Leftrightarrow \hat{\mathcal{R}}_0^C > 1 \ (or <). \end{aligned}$$

By the same argument above, one can also show that the threshold conditions $\hat{\mathcal{R}}_0^L$ and $\mathcal{R}_0^L$ are also equivalent.

With the same argument, we can also establish the following result:

Lemma VII.2 *Assume $\tilde{r} = 0$. Let*

$$\hat{\mathcal{R}}_{inv}^L := \frac{\phi S_C^+(\beta\eta - (\eta + d))}{\mu(\eta + d)} \text{ and } \hat{\mathcal{R}}_{inv}^C := \frac{\tilde{\phi} S_L^+(\alpha - \eta)}{\mu + \tilde{d}}.$$

Then, for all $i \in \{L, C\}$, the invasion fitness quantity $\mathcal{R}_{inv}^i$ is equivalent to $\hat{\mathcal{R}}_{inv}^i$, respectively.

Proof VII.4 (Proof of Theorem VII.9) *If $\tilde{r} = 0$, then the chronic susceptible equilibrium is*

$$S_C^+ = \frac{\mu\tilde{d}}{\tilde{\phi}(\alpha - \tilde{d})} = \frac{S_0}{\hat{\mathcal{R}}_0^C}, \tag{18}$$

where $\hat{\mathcal{R}}_0^C = \dfrac{\tilde{\phi} S_0(\alpha - \eta)}{\mu + \tilde{d}}$. Recall that lytic invasion conditions is:

$$\hat{\mathcal{R}_{inv}^L} = \frac{\phi S_C^+(\beta\eta - (\eta + d))}{\mu(\eta + d)}. \tag{19}$$

Substituting (18) into the equation (19), we obtain $\mathcal{R}_{inv}^L = \dfrac{\hat{\mathcal{R}}_0^L}{\hat{\mathcal{R}}_0^C}$. Therefore $\mathcal{R}_{inv}^L > 1$ if and only if $\hat{\mathcal{R}}_0^L > \hat{\mathcal{R}}_0^C$ (which holds if and only if $\mathcal{R}_0^L > \mathcal{R}_0^C$.) By the same argument, we can also show $\mathcal{R}_0$ maximization for chronic virus invasion.

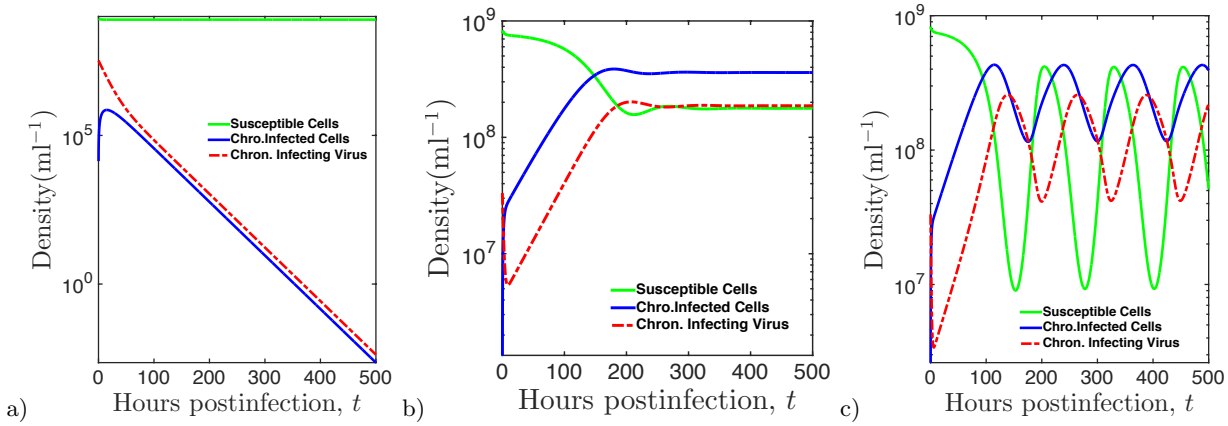

FIG. 10: Dynamics of the chronic-subsystem (III) with susceptible hosts, $S(t)$, chronically infected hosts, $C(t)$, and chronically infecting free viruses, $V_C(t)$, at time t. a) Infection dies out and population density converges to infection-free equilibrium, $\mathcal{E}_0$. b) Population density size converges to positive interior equilibrium, $\mathcal{E}_C^+$. c) The system displays Hopf bifurcation: the interior equilibrium, $\mathcal{E}_C^+$, loses its stability and the system exhibits sustained oscillations. Common parameters for the dynamics are given in the Table III. The initial virus and host densities are $V_0^C = 0.04 \times S_0$ viruses/ml, $S_0 = 8.3 \times 10^8$ hosts/ml. For part (a) $\tilde{\phi} = 0.5 \times 10^{-11}$, part (b) $\tilde{\phi} = 0.5 \times 10^{-9}$ and part (c) $\tilde{\phi} = 0.1 \times 10^{-8}$.

TABLE IV: Infection and Invasion Regions

Region	$\mathcal{R}_0^L$	$\mathcal{R}_0^C$	$\mathcal{R}_{inv}^L$	$\mathcal{R}_{inv}^C$	Infection	Invasion
I	<1	<1	–	–	No infection	No invasion
II	<1	>1	<1	–	Only chronic	No invasion
III	<1	>1	>1	–	Only chronic	Lytic invades
IV	>1	<1	–	>1	Only lytic	Chronic invades
V	>1	<1	–	<1	Only lytic	No invasion
VI	>1	>1	<1	>1	Both infection	Chronic invades
VII	>1	>1	<1	<1	Both infection	No invasion
$VIII$	>1	>1	>1	>1	Both infection	Both invades
IX	>1	>1	>1	<1	Both infection	Lytic invades

Acknowledgments

The authors thank Guanlin Li for helpful comments and feedback on the manuscript. JSW acknowledges support from NSF Award DEB-1342876.

[1] Beretta, Edoardo and Kuang, Yang (1998) Modeling and analysis of a marine bacteriophage infection. *Mathematical biosciences* 149 (1): 57–76.

[2] Gulbudak, H and Weitz, JS (2016) A Touch of Sleep: Biophysical Model of Contact-mediated Dormancy of Archaea by Viruses. *Proceedings of the Royal Society B* 283(1839):20161037.

[3] Childs, Lauren M, Held, Nicole L ,Young, Mark J, Whitaker, Rachel J, Weitz, Joshua S (2012)Multiscale Model of CRISPR-Induced Coevolutionary Dynamics: Diversification at the Interface of Lamarck and Darwin. *Evolution* 66(7):2015–2029.

[4] Gandon, S, Vale, PF (2014) The evolution of resistance against good and bad infections. *Journal of evolutionary biology* 27(2):303–312.

[5] Weitz, Joshua S (2016) Quantitative Viral Ecology: Dynamics of Viruses and Their Microbial Hosts. *Princeton University Press*

[6] Smith, Hal L and De Leenheer, Patrick (2003)Virus dynamics: a global analysis. *SIAM Journal on Applied Mathematics* 63(4):1313–1327.

[7] Maslov, S, Sneppen, K (2015) Well-temperate phage: optimal bet-hedging against local environmental collapses. *Scientific Reports* 5:10523.

[8] Levin, B. R., Stewart, F. M., Chao, L. (1977) Resource-limited growth, competition, and predation: a model and experimental studies with bacteria and bacteriophage. *American Naturalist*:3–24.

[9] Chibani-Chennoufi, Sandra and Bruttin, Anne and Dillmann, Marie-Lise and Brüssow, Harald (2004) Phage-host interaction: an ecological perspective *Journal of bacteriology* 186(12):3677–3686.

[10] Adams, Mark Hancock and others (1959) Bacteriophages. *New York (& London): Inter-science Publishers.*

[11] Bautista, Maria A and Zhang, Changyi and Whitaker, Rachel J (2015) Virus-Induced Dormancy in the Archaeon Sulfolobus islandicus. *MBio 6 (2). [Am Soc Microbiol]* e02565–14.

[12] Campbell, A (1961) Conditions for the Existence of Bacteriophage. *Evolution 15 (2). [Society for the Study of Evolution, Wiley]* 15365. doi:10.2307/2406076.

[13] Rakonjac, Jasna (2012) Filamentous bacteriophages: biology and applications. *eLS.*

[14] De Paepe M, Tournier L, Moncaut E, Son O, Langella P, Petit M-A (2016) Carriage of ? Latent Virus Is Costly for Its Bacterial Host due to Frequent Reactivation in Monoxenic Mouse Intestine. *PLoS Genet* 12(2): e1005861. doi:10.1371/journal.pgen.1005861

[15] Díaz-Muñoz, Samuel L and Koskella, Britt (2014) Bacteria-phage interactions in natural environments. *Adv Appl Microbiol* 89:135–83.

[16] Lin, L, Bitner, R, Edlin, Gordon (1977) Increased reproductive fitness of Escherichia coli lambda lysogens. *Journal of virology* 21(2):554–559.

[17] Harcombe, William Russell (2009) The evolutionary ecology of model microbial communities. *The University of Texas at Austin Library*

[18] Fortier, Louis-Charles and Sekulovic, Ognjen (2013) Importance of prophages to evolution and virulence of bacterial pathogens. *Virulence* 4 (5):354–365.

[19] Carlton, Richard M (1999) Phage therapy: past history and future prospects. *Archivum immunologiae et therapiae experimentalis* 47:267–274.

[20] Wiggins, Bruce Arthur and Alexander, MARTIN (1985) Minimum bacterial density for bacteriophage replication: implications for significance of bacteriophages in natural ecosystems. *Applied and Environmental Microbiology* 49(1):19–23.

[21] Karlsson,C (2004) The Biology of Filamentous Phage Infection: Implications for Display Technology *Publisher Lund Univ.* ISBN 9174220640, 9789174220643.

[22] Gulbudak, Hayriye and Martcheva, Maia. (2013)Forward hysteresis and backward bifurcation caused by culling in an avian influenza model *Math. Biosci.* 246(1): 202-212.

[23] Van den Driessche, P and Watmough, J (2002) Reproduction numbers and sub-threshold endemic equilibria for compartmental models of disease transmission. *Mathematical biosciences* 180(1):29–48.

[24] Diekmann, O. ,Heesterbeek, J. A. P. , Metz, J.A.J. (1990) On the definition and the computation of the basic reproduction ratio R 0 in models for infectious diseases in heterogeneous populations. *Journal of mathematical biology* 28(4):365–382.

[25] Hurford, A, Cownden, D, Day, T (2010) Next-generation tools for evolutionary invasion analyses. *Journal of the Royal Society Interface* 7(45):561–571.

[26] Bremermann, H. J., Thieme, H. R. (1989) A competitive exclusion principle for pathogen virulence. *Journal of mathematical biology* 27(2):179–190.

[27] Feng, Z., Velasco-Hernández, J. X. (1997) Competitive exclusion in a vector-host model for the dengue fever. *Journal of mathematical biology* 35(5):523–544.

[28] Martcheva, M., Nuno, M., Feng, Z., Castillo-Chavez, C. (2008) Mathematical Models of Influenza: The Role of Cross-Immunity, Quarantine and Age-Structure, Lecture Notes in Mathematics, Mathematical Epidemiology, (Fred Brauer, Pauline van den Driessche, Jianhong Wu, Eds.). *Springer-Verlag, Berlin*(1945): 349-364.

[29] De-Lian Q., Xue-Zhi L., Ghosh, M. (2012) Coexistence of Strains induced by Mutation. *International Journal of Biomathematics*:05:03.

[30] Nowak, M. A., May, R. M. (1994) Superinfection and the evolution of parasite virulence. *Proceedings: Biological Sciences*255:81–89.

[31] May, R. M., Nowak, M. A. (1995) Coinfection and the evolution of parasite virulence. *Proc R Soc* 261:209–215.

[32] Pugliese, A. (1995) Pathogen coexistence induced by density-dependent host mortality. *Journal of theoretical biology*177(2):159–166.

[33] Gulbudak, H., Ponce J., Martcheva M. (2016) Coexistence Caused by Culling In a Two-Strain Avian Influenza Model *Nova Science Publishers*108:153–182.

[34] Faeth, S. H., Hadeler, K. P.,Thieme, H. R. (2007) An apparent paradox of horizontal and vertical disease transmission. *Journal of biological dynamics*1(1):45–62.

[35] Jones, E. O., White, A., Boots, M. (2007) Interference and the persistence of vertically transmitted parasites. *Journal of theoretical biology*246(1):10–17.

[36] Lipsitch, M., Siller, S. and Nowak, M. A. (1996) The evolution of virulence in pathogens with vertical and horizontal transmission. *Evolution*:1729–1741.

[37] Ewald, P. W. (1993) The evolution of virulence. *Scientific*

*American*268(4):86–93.

[38] Yoon, C. K. (1993) What might cause parasites to become more virulent. *Science*259(5100):1402–1402.

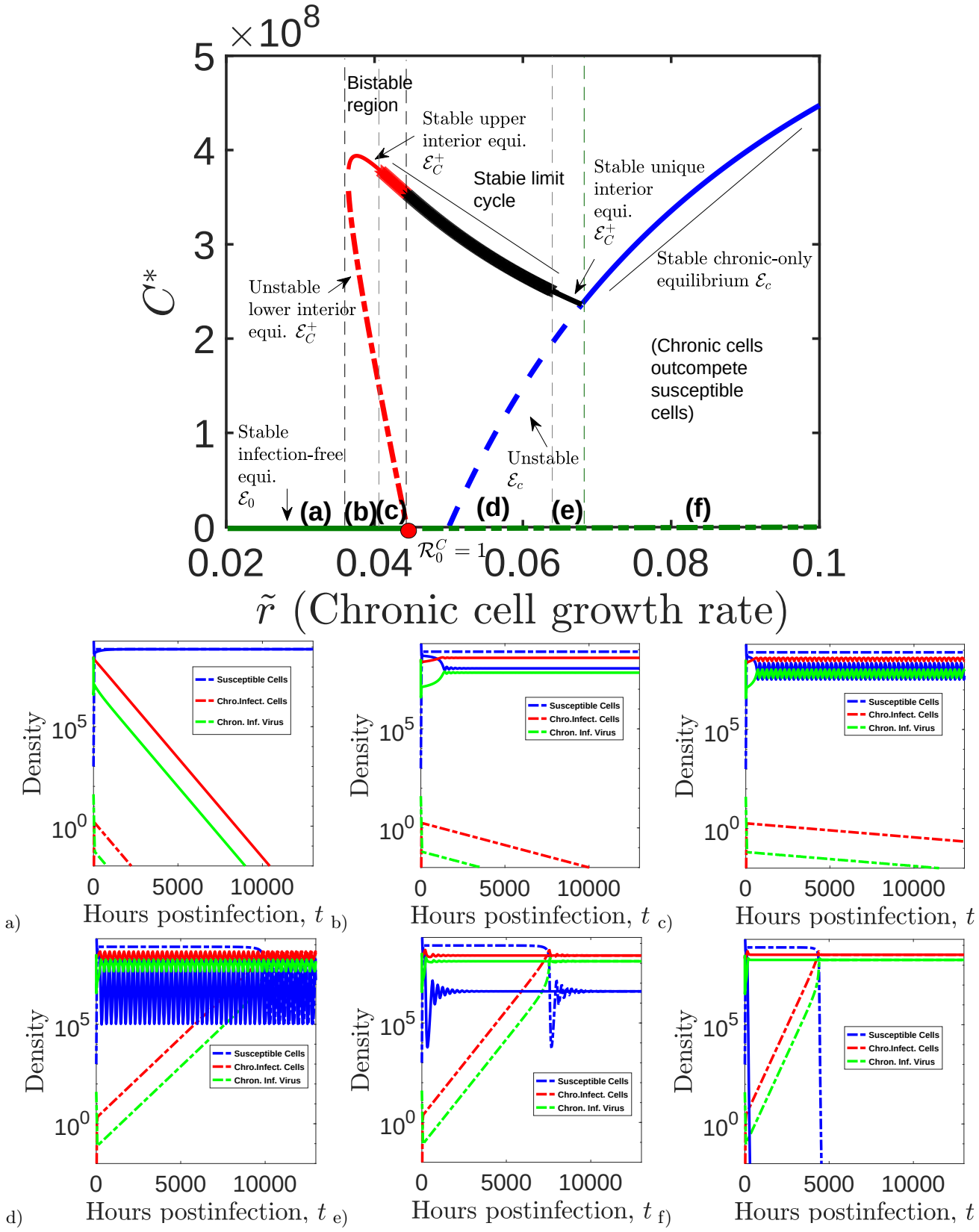

FIG. 11: Corresponding distinct time-dependent solutions of the chronic subsystem derived from varying bifurcation parameter,$\tilde{r}$. a) *Region (a):* Stable DFE with $\tilde{r} = 0.025$. b) *Region (b):* Bistability with stable positive EE, $\mathcal{E}_C^+$, with $\tilde{r} = 0.04$. c) *Region (c):* Bistability with stable limit cycle with $\tilde{r} = 0.043$. d) *Region (d):* Stable limit cycle with $\tilde{r} = 0.06$. e) *Region (e):* Stable positive EE, $\mathcal{E}_C^+$, with $\tilde{r} = 0.065$. f) *Region (f):* Stable chronic-only equilibrium, $\mathcal{E}_c$, with $\tilde{r} = 0.08$. The initial virus and host densities are: $S_0 = 8.3 \times 10^9$ hosts/ml & $V_0^C = 0.04 \times S_0$ viruses/ml (high density); $S_0 = 10^3$ hosts/ml, & $V_0^C = 0.04 \times S_0$ viruses/ml (low density), $C_0 = 0$ hosts/ml.

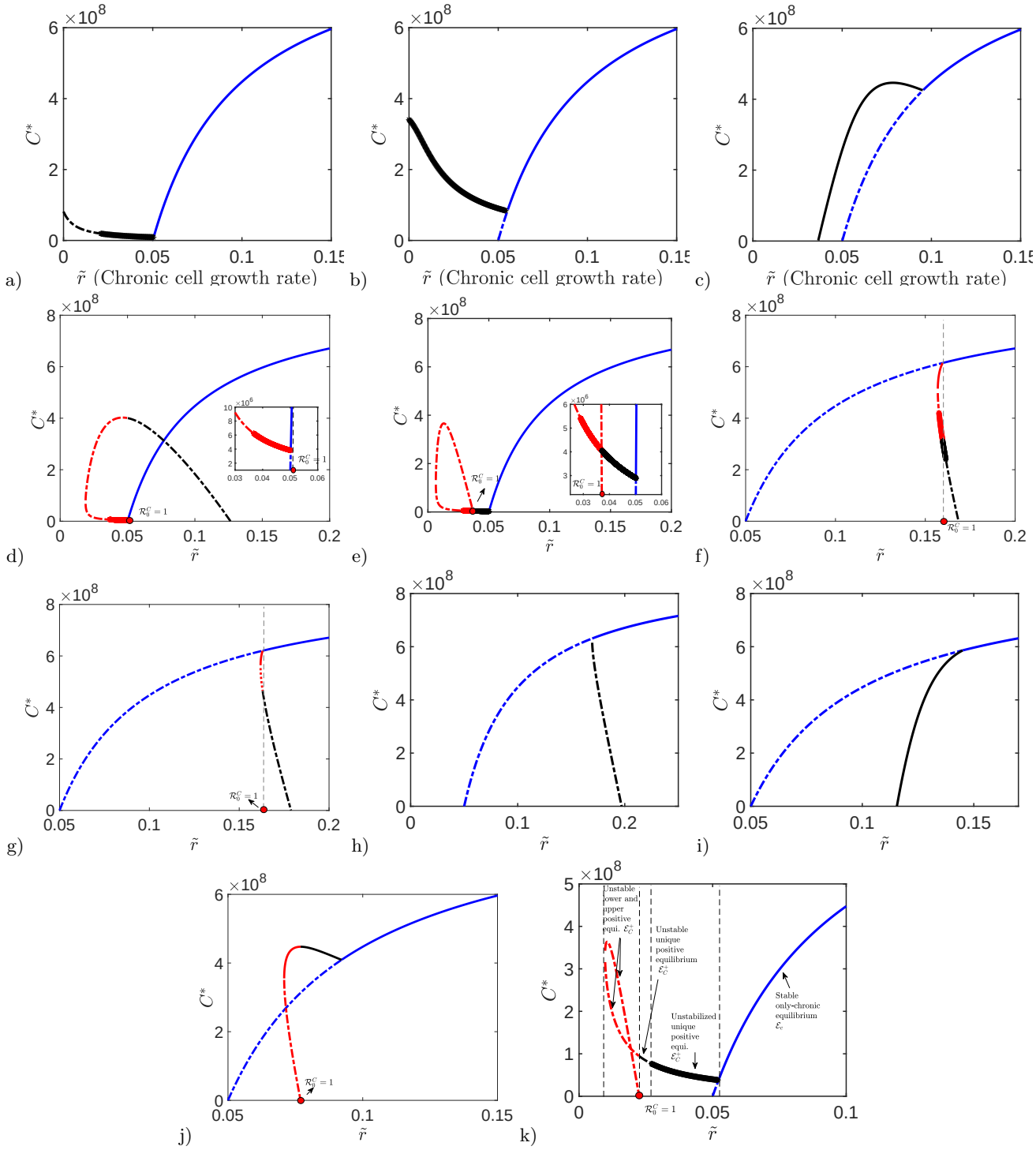

FIG. 12: Additional bifurcation dynamics of chronic-only system (III) with varying values of the model parameters $\tilde{r}$ and $\tilde{\phi}$. The solid (dashed) lines represent stable (unstable) equilibrium. The black lines are the unique equilibrium. The red lines shows the region, where bistability occurs (except the figure in part (k)) with stable infection-free equilibrium, $\mathcal{E}_0$ (not displayed in these figures) and the blue lines represent chronic-only equilibrium, $\mathcal{E}_c$. The parameter values used here are as follows: a) $\alpha = 1/18,\ \tilde{\phi} = 5 \times 10^{-8}$, b) $\alpha = 1/18,\ \tilde{\phi} = 5 \times 10^{-9}$, c) $\alpha = 1/18,\ \tilde{\phi} = 5 \times 10^{-10}$, d) $\alpha = 1/29,\ \tilde{\phi} = 1.95 \times 10^{-7}$, e) $\alpha = 1/22,\ \tilde{\phi} = 1.95 \times 10^{-7}$, f)$\alpha = 1/22,\ \tilde{\phi} = 2 \times 10^{-10}$, g) $\alpha = 1/23,\ \tilde{\phi} = 2 \times 10^{-10}$, h) $\alpha = 1/25,\ \tilde{\phi} = 2 \times 10^{-10}$, i) $\alpha = 1/18,\ \tilde{\phi} = 2 \times 10^{-10}$, j)$\alpha = 1/21,\ \phi 2 = 2 \times 10^{-9.5}$, k) $\alpha = 1/21,\ \tilde{\phi} = 1.35 \times 10^{-8}$, The rest of the parameter values are identical to the ones in Table I.

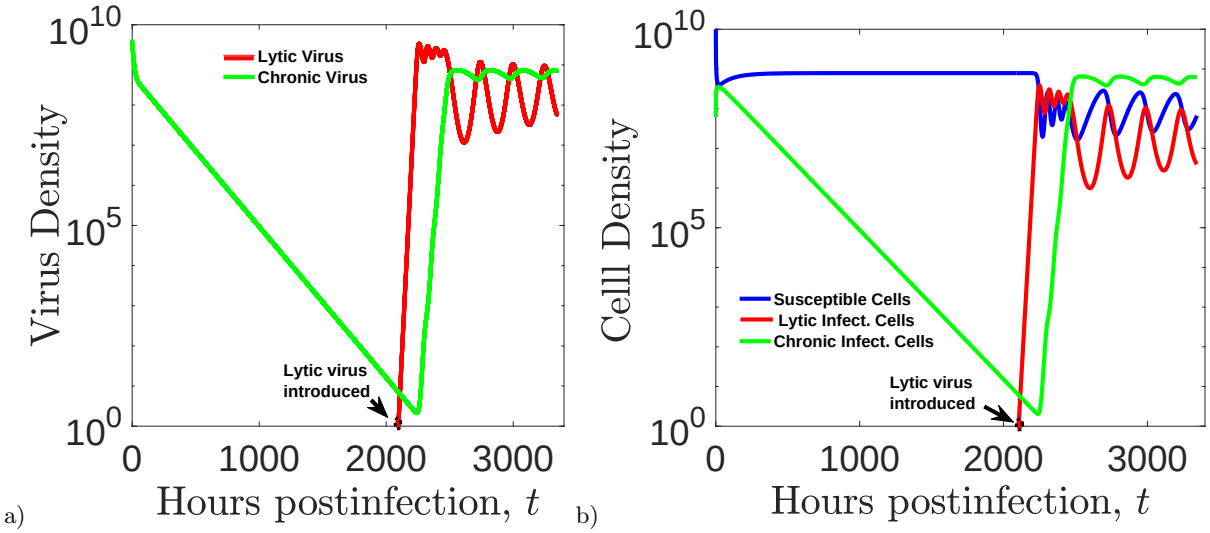

FIG. 13: a)Changing cell population dynamics after lytic virus introduction b)Changing virus population dynamics after lytic virus introduction a)"Rescue" of chronically infecting viruses by lytic viruses b) "Rescue" of chronically infected cells by lytic viruses.